energies

MDPI

Review

Direct Air Capture Using Pyrolysis and Gasification Chars: Key Findings and Future Research Needs

Wojciech Jerzak [1,*], Bin Li [2], Dennys Correia da Silva [3] and Glauber Cruz [4]

[1] Faculty of Metals Engineering and Industrial Computer Science, AGH University of Krakow, Mickiewicza Av. 30, 30-059 Krakow, Poland
[2] School of Engineering, Anhui Agricultural University, 130 Changjiang West Road, Hefei 230036, China; libin198520@126.com
[3] Postgraduate in Chemical Engineering, Department of Chemical Engineering, Federal University of Rio Grande do Norte, Natal 59072-970, Rio Grande do Norte, Brazil; dennys.silva19@gmail.com
[4] Thermochemical Processes and Systems Laboratory (LPSisTer), Department of Mechanical Engineering, Federal University of Maranhão, Avenida dos Portugueses, 1966, São Luís 65080-805, Maranhão, Brazil; cruz.glauber@ufma.br
* Correspondence: wjerzak@agh.edu.pl; Tel.: +48-12-6172636

Abstract

Direct Air Capture (DAC) is gaining worldwide attention as a negative emissions strategy critical to meeting climate targets**.** Among emerging DAC materials, pyrolysis chars (PCs) and gasification chars (GCs) derived from biomass present a promising pathway due to their tunable porosity, surface chemistry, and low-cost feedstocks. This review critically examines the current state of research on the physicochemical properties of PCs and GCs relevant to CO_2 adsorption, including surface area, pore structure, surface functionality and aromaticity. Comparative analyses show that chemical activation, especially with KOH, can significantly improve CO_2 adsorption capacity, with some PCs achieving more than 308 mg/g (100 kPa CO_2, 25 °C). Additionally, nitrogen and sulfur doping further improves the affinity for CO_2 through increased surface basicity. GCs, although inherently more porous, often require additional modification to achieve a similar adsorption capacity. Importantly, the long-term stability and regeneration potential of these chars remain underexplored, but are essential for practical DAC applications and economic viability. The paper identifies critical research gaps related to material design and techno-economic feasibility. Future directions emphasize the need for integrated multiscale research that bridges material science, process optimization, and real-world DAC deployment. A synthesis of findings and a research outlook are provided to support the advancement of carbon-negative technologies using thermochemically derived biomass chars.

Keywords: biomass-derived sorbents; biochar activation; carbon capture materials; CO_2 adsorption; surface functionality

Academic Editor: Alberto Pettinau

Received: 8 July 2025
Revised: 27 July 2025
Accepted: 31 July 2025
Published: 3 August 2025

Citation: Jerzak, W.; Li, B.; Silva, D.C.d.; Cruz, G. Direct Air Capture Using Pyrolysis and Gasification Chars: Key Findings and Future Research Needs. *Energies* **2025**, *18*, 4120. https://doi.org/10.3390/en18154120

1. Background and Importance of Atmospheric CO_2 Mitigation

According to the latest global report on CO_2 emissions by the International Energy Agency [1], worldwide CO_2 emissions continue to increase despite ongoing mitigation efforts. This upward trend has led to a record high atmospheric CO_2 concentration of 424.6 ppm in 2024, approximately 3.5 ppm higher than in 2023 [2]. Figure 1 shows that the at-

mospheric CO_2 concentration increased by 25.8 ppm between 2014 and 2024. This alarming rise underscores the urgent need for innovative strategies to reduce atmospheric CO_2 levels, beyond merely reducing emissions at their source.

This review aims to bridge critical knowledge gaps by offering a comprehensive and structured analysis of pyrolysis and gasification chars as adsorbents for direct air CO_2 capture. Although many previous reviews have focused on carbon materials in general, they often lack detailed comparisons between pyrolysis and gasification chars in terms of their physicochemical properties, CO_2 adsorption capacity, and process limitations. This work distinguishes itself by integrating mechanistic insights (e.g., surface chemistry, porosity development, and aromaticity) with process-level considerations (e.g., energy requirements, scalability, and real-world application challenges). By combining a comparative perspective with a focus on direct air capture, this review provides a timely resource to guide future material design and system integration strategies in the context of climate mitigation.

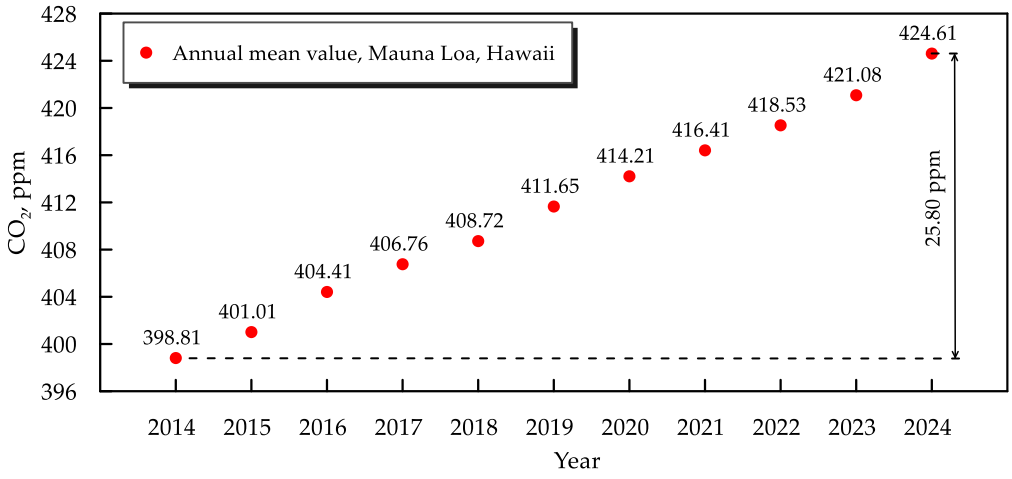

Figure 1. Increase in global average atmospheric CO_2 concentration during the past decade (2014–2024). Source: Mauna Loa Observatory [2].

To guide this review, we formulate the following research questions:

(1) What are the key physicochemical properties and modification strategies that enhance the CO_2 adsorption capacity of the pyrolysis and gasification chars?

(2) What are the major knowledge gaps and future research needs that must be addressed to enable the large-scale implementation of char-based materials in direct air capture systems?

2. Overview of Direct Air Capture Technologies and Materials

Direct air capture (DAC) is a promising approach to mitigating excess atmospheric CO_2 by capturing it directly from ambient air. DAC refers to the process of extracting CO_2 directly from the ambient air and storing it in geological formations for long-term sequestration [3]. Due to the low concentration of CO_2 in the ambient air (≈425 ppm), DAC requires considerable energy input and depends on advanced sorbent materials with high selectivity and affinity for CO_2 under such dilute conditions. Various DAC technologies have been developed and evaluated for the mitigation of atmospheric CO_2. An overview of DAC techniques is presented in Table 1.

Table 1. Overview of direct air capture technologies.

Type	Technology	Mechanism and Key Features	Refs.
Liquid-based	Alkaline Solvents (KOH, NaOH)	CO_2 reacts with an alkaline solution to form carbonates; regenerated by calcination.	[4,5]
Liquid-based	Amino Acid Solution	CO_2 forms bicarbonates; regeneration through mild heating; low volatility and energy demand.	[6]
Solid-based	Amine-Functionalized Solids	CO_2 chemically absorbed by amines on supports (e.g., alumina, resins).	[7,8]
Solid-based	Temperature-Vacuum Swing Adsorption (TVSA)	CO_2 is physically adsorbed at room temperature and is desorbed by heating and vacuum.	[9,10]
	Chars/Activated Carbons	Porous carbon materials (e.g., doped chars); adsorption via surface area and functionality.	[11]
	Metal-Organic Frameworks (MOFs)	Crystalline porous materials with a tunable structure and high CO_2 selectivity.	[12]
	Zeolites	Selective CO_2 separation using microporous crystalline structures.	[13]
Electrochemical	Electro-Swing Adsorption	Redox-active materials bind/release CO_2 via voltage control under mild conditions.	[14]
	Electrochemical Cells	CO_2 capture and conversion using ion transport through electrochemical cells	[15]
Hybrid	TVSA + Dehumidification	The pre-drying air improves the CO_2 capture efficiency in TVSA systems.	[16]
	Passive Air Contactors	Wind-driven flow over solid sorbents (e.g., amine-grafted monoliths); low energy demand.	[17]

2.1. Liquid-Based Absorption

Liquid-based DAC technologies employ aqueous solvents to capture CO_2 efficiently, even from highly diluted air streams. These systems, which use alkaline solutions, such as KOH [5] and NaOH [4], have demonstrated considerable capture capacities and economic viability. General reactions (1) through (4) describe the sequential steps of the CO_2 capture process using KOH, which takes place in the air contactor, causticizer, calciner, and slaker units, respectively [18].

$$CO_{2(g)} + 2KOH_{(aq)} \rightarrow H_2O_{(l)} + K_2CO_{3(aq)} \quad (1)$$

$$K_2CO_{3(aq)} + Ca(OH)_{2(aq)} \rightarrow 2KOH_{(aq)} + CaCO_{3(s)} \quad (2)$$

$$CaCO_{3(s)} \rightarrow CaO_{(s)} + CO_{2(g)} \quad (3)$$

$$CaO_{(s)} + H_2O_{(l)} \rightarrow Ca(OH)_{2(aq)} \quad (4)$$

KOH-based systems can achieve CO_2 capture of up to 1.1 million tons per year, with potential economic offsets from CO_2 utilization [5], while NaOH–Na_2CO_3 systems offer high mass transfer coefficients, but require optimized concentrations to balance absorption efficiency and solubility dynamics [10]. The KOH production process is more expensive, making it a costlier option compared to NaOH [19]. Recent advances have also explored the use of aqueous amino acid solvents, such as potassium sarcosinate, in combination with 3D-printed gyroidal structures that improve gas–liquid contact and reduce pressure drop [6]. These systems offer CO_2 capture performance comparable to that of conventional packings, while benefiting from improved stability, lower volatility, and reduced energy demand for regeneration. According to Kiani et al. [20], potassium salts of sarcosine and proline are among the most promising DAC solvents, due to their high CO_2

absorption rates and superior oxidative stability compared to monoethanolamine. However, due to their limited thermal stability, further process optimization is needed to enable regeneration under milder desorption conditions. Kiani et al. [21] developed a second generation DAC system using an amine-based liquid, called the mist contactor, which is expected to reduce CO_2 capture costs to USD 68 per ton by 2035, at a capacity of 1 million tons of CO_2 per year.

2.2. Solid-Based Absorption

Solid sorbents impregnated with amines have received substantial attention because of their high selectivity and tunable adsorption properties. These hybrid materials can be customized by physical impregnation (Class I) [22], covalent grafting (Class II) [22], or in situ polymerization (Class III) [23] to optimize the loading of amines and ensure long-term stability. The performance of these sorbents depends not only on the support structure, but also on the type of amine used, with optimized blends of primary, secondary and tertiary amines that offer a compromise between fast kinetics and resistance to degradation [24].

Amine-impregnated alumina supports (e.g., γ-Al_2O_3 with poly(ethyleneimine) or tetraethylenepentamine, TEPA) demonstrate promising CO_2 adsorption capacity at ambient and sub-ambient temperatures, reaching up to 1.8 mmol of CO_2/g [8]. Similarly, polyethyleneimine loaded polymeric resins exhibit high CO_2 capacities, excellent thermal stability, and durability over multiple cycles, particularly under humid conditions, which can improve performance up to 130 mg/g [7].

2.3. Solid-Based Adsorption

Solid-sorbent DAC systems operate by passing ambient air through chambers filled with materials that can capture CO_2 from the air. In this process, air is typically pushed through the system using fans, and as it flows over the solid sorbent, CO_2 binds to the material at room temperature. The cleaned CO_2-depleted air then exits the system. Such systems operate cyclically, with the sorbent regenerated, typically by heating or vacuum, to release the captured CO_2 [25]. Air contactors in DAC systems include fixed beds, monolithic structures [26], and fluidized beds [27], depending on system design and scale.

Temperature-Vacuum Swing Adsorption (TVSA) is a widely used regeneration method for solid-sorbent-based DAC systems. In this process, CO_2 from the ambient air is first captured at room temperature as it passes through a solid sorbent bed. To release captured CO_2, the system applies both heating and pressure reduction (moderate vacuum) to efficiently desorb CO_2. This combination allows efficient desorption while avoiding the need for the extremely deep vacuum levels required in pressure-swing systems. Metal–organic framework (MOF) sorbents have demonstrated high productivity and energy efficiency in TVSA cycles (≈5.5 h), with additional potential for thermal optimization through integrated heating and vacuum management [10]. Pilot-scale implementations using steam-assisted TVSA systems have achieved stable operation and CO_2 production of 1.3 kg/day, with energy use ranging from 14.5 to 16.4 GJ per ton of CO_2 [9].

Chars, metal-organic frameworks (MOFs), and zeolites are three distinct classes of porous materials explored for the capture of CO_2 from air, each offering unique structural and functional characteristics. Ultimately, the choice between these materials depends on trade-offs between performance, cost, moisture tolerance, and regeneration efficiency. Chars are carbon-rich solids derived from the pyrolysis or gasification of biomass. According to the EU Renewable Energy Directive (RED II) [28], some waste materials can be legally classified as biomass, provided they meet specific quality criteria and are intended for recovery, based on technological and environmental documentation.

Char adsorbents prepared from sewage sludge have shown potential for DAC, especially when produced at high pyrolysis temperatures and modified by amine doping [11]. These materials provide a sustainable pathway for CO_2 capture while allowing waste valorization. MOFs represent a more advanced class of crystalline materials composed of metal nodes and organic linkers. They offer highly tunable structures, large surface areas, and a variety of adsorption mechanisms, including open metal sites and functional group interactions [29]. However, their high production costs and sensitivity to moisture remain barriers to widespread DAC deployment. MOFs have been extensively studied for their tunable pore structures and strong electrostatic interactions, which drive selective CO_2 adsorption at low pressures. Frameworks such as ZIF-69 and CAU-10 demonstrate excellent uptake due to confined pore sizes and polar functional groups that facilitate high-affinity CO_2 binding [12]. Zeolites, on the other hand, are crystalline aluminosilicates with well-defined pore structures and a strong affinity for polar molecules such as CO_2 due to their negatively charged frameworks [30]. Although low-cost and abundant, zeolites suffer performance losses in humid environments and often require air pre-drying. Engineered variants such as Fe-doped 13X zeolite exhibit faster kinetics and greater CO_2 adsorption capacity under ambient conditions [13]. This modification improves the selectivity of CO_2 while maintaining thermal stability and low-pressure operability.

2.4. Electrochemically (Liquid and Solid Sorbent)

Electrochemical technologies for DAC offer a promising alternative to thermal regeneration methods by allowing CO_2 capture and release through controlled redox reactions under mild conditions. They generally operate under ambient conditions, allowing seamless integration with renewable energy systems. Two main approaches are used: (1) direct electrochemical capture, where redox-active sorbents, such as quinones or organic dyes bind or release CO_2 in response to an applied voltage [14]; and (2) electrochemically mediated competitive complexation, where an external redox-active agent modulates the sorbent's affinity for CO_2 [31]. A third approach uses electrochemical cells with anion exchange membranes to transport carbonate or bicarbonate ions, allowing CO_2 capture and separation on the output side [15]. Although still in development, these methods have shown significant reductions in energy consumption compared to traditional thermal processes, offering potential for scalable, low-energy DAC systems.

Electro-swing adsorption systems using NR/NRH_2 redox pairs exhibit reversible operation and low energy demand (≈65 kJe/mol CO_2) although the design of the absorption unit still constrains stability and efficiency [14]. Electrochemical cells using anion exchange membranes have reached current densities of 326 mA/cm^2 at 1.2 V and CO_2 capture efficiencies of up to 95.7%, particularly when humidity and electrode structure are optimized [15].

2.5. Hybrid Systems

Hybrid DAC systems, which combine temperature–vacuum swing adsorption (TVSA) with predehumidification methods (e.g., condensation or solid desiccants), offer enhanced energy efficiency and cost-effectiveness in humid environments. Techno-economic analyses show that performance is optimized at 40.0% relative humidity, with levelized DAC costs reduced to USD 194–200 per ton of CO_2 and thermal energy use reduced to 15.5 GJ/ton [16]. Furthermore, passive air contactors equipped with amine-grafted, alumina-coated monoliths provide low pressure drop and rapid CO_2 adsorption kinetics. Their uniform functionalization and compatibility with industrial substrates make them promising for large-scale DAC deployment, however, further investigation is needed to assess moisture tolerance and long-term operational stability [17].

2.6. Relevance of Carbon-Based Solid Adsorbents for DAC

Among the various DAC approaches, solid adsorbents, particularly low-cost carbon-based materials, have emerged as a major research hotspot. Compared to liquid solvents or metal–organic frameworks (MOFs), solid adsorbents offer several advantages, including lower regeneration energy, better thermal and chemical stability, and reduced sensitivity to contaminants such as moisture or trace gases [32–34]. Furthermore, carbon materials derived from biomass are abundant, inexpensive, and tunable in terms of porosity and surface functionality, making them attractive candidates for scalable, low-cost DAC systems. These features position pyrolysis and gasification chars as a promising class of sorbents for next-generation carbon removal technologies.

3. Pyrolysis and Gasification Chars as CO_2 Sorbents

Carbon-based materials, such as pyrolysis and gasification chars, are increasingly recognized as promising solid sorbents for CO_2 capture. They are low cost [35], resistant to moisture [34], and thermally stable [36]. Their renewable origin, adjustable porosity, and diverse surface functionalities make them attractive candidates for DAC applications [25]. Pyrolysis char (PC), commonly known as biochar, and gasification char (GC), are solid carbonaceous residues derived from the thermochemical conversion of biomass. However, they differ markedly in their formation mechanisms, process conditions, and resulting physicochemical characteristics. Pyrolysis is carried out under an oxygen deficient atmosphere at temperatures ranging from 300 °C [33] to 1200 °C [37], thermally decomposing biomass into char (PC), bio-oil and non-condensable gases. PC forms mainly through the aromatic stabilization of lignin-derived structures through depolymerization, dehydration, and aromatization [38]. The yield and quality of PC are influenced by temperature [39], feedstock type [40], and moisture content [41]. On the contrary, gasification operates at higher temperatures (700–1500 °C) in a partially oxidizing atmosphere (e.g., air, steam, or CO_2), primary producing syngas (H_2, CO, CO_2) and a small amount (≈10%) of GC [37]. The GC results form partial oxidation and secondary cracking of organic matter.

3.1. Physicochemical Properties

This section describes the key physicochemical properties of pyrolysis and gasification chars that govern their CO_2 adsorption capacity, including surface area, porosity, ash content and carbon structure.

3.1.1. Specific Surface Area

The specific surface area (SSA) of char materials, commonly measured using the Brunauer–Emmett–Teller (BET) method, is a fundamental parameter governing the adsorption capacity of CO_2. Quantifies the total surface area available for adsorption per gram of material and is particularly relevant for microporous solids such as PCs or GCs. Table 2 summarizes the BET surface area of various PCs under different thermal and activation conditions. In general, higher pyrolysis temperatures result in an increased surface area. For example, bamboo-derived chars reached 89–350 m^2/g in a temperature range of 350–950 °C [42]. However, this increase plateaus or even declines at excessively high temperatures or extended residence times. It has been observed that prolonging residence time beyond 120 min at high temperatures can result in structural collapse or pore sintering, reducing the surface area of BET [42].

Chemical activation, especially with KOH, significantly increases the surface area. For example, PC from a mixture of pine wood and sewage sludge reached an exceptional 2623 m^2/g after activation at 700 °C [33]. Other activated PCs, derived from garlic peel,

whitewood, and pine sawdust, also exhibited surface areas above 900 m^2/g [43–45]. In particular, the maximum surface area does not always correspond to the maximum CO_2 adsorption capacity [43]. The mass ratio of the activating agent to chars a critical factor [46,47]; higher ratios tend to improve porosity, but overly high doses can reduce the yield or damage the structure.

Table 2. Effect of biomass types, temperature (T), residence time (RT), and activation conditions on the specific surface area (SSA) of PCs.

Biomass Types	Pyrolysis		Activation				BET SSA, m^2/g	Refs.
	T, °C	RT, min	Method	T, °C	RT, min	C:A [(a)]		
70% Pine Wood-30% Sewage Sludge	600	240	Raw	-	-	-	182	[33]
	700	240					223	
	800	240					150	
	300	240	KOH	600	240	1:1	703	
	300	240	KOH	700	240	1:1	2623	
	300	240	KOH	800	240	1:1	2047	
Bamboo impregnated with H_2SO_4	350	120	-	-	-	-	89	[42]
	550	120					140	
	750	120					229	
	950	60					310	
	950	120					350	
	950	180					346	
	950	240					314	
Garlic Peel	400	120	Raw	-	-	-	306	[43]
			KOH	600	60	1:2	947	
			KOH	700	60	1:2	1179	
			KOH	800	60	1:2	1262	
Whitewood	500	-	Steam	700	85	1:0.94	840	[44]
			CO2	890	100	1:8.7	820	
			KOH	775	120	1:1.23	1400	
Pine Sawdust	800	5	Raw	-	-	-	368	[45]
			Steam	850	25	1:0.4	701	
			KOH	850	60	1:3	1375	
Wood Pellet	1200	-	Raw	-	-	-	161	[48]
			Steam	550	60	1:2.5	307	
			CO_2	550	60	1:16.7	287	
			$ZnCl_2$	550	60	1:1	4.56	
			H_3PO_4	550	60	1:1	3.19	
			KOH	550	60	1:1	439	
Solid digestate	600	9	Raw	-	-	-	6	[49]
	700						5	
	800						16	
	900						63	

[(a)] C:A is the ratio of pyrolysis char to the activating agent. For activating agents in the solid state, this refers to the mass ratio of pyrolysis char to the activating agent. For steam as the activating agent, it is the mass ratio of pyrolysis char to steam. For CO_2 as the activating agent, it refers to the ratio of the mass (in grams) of pyrolysis char to the volume of CO_2 (in cm^3).

As shown in Table 3, GCs often exhibit higher BET surface areas in their non-activated form compared to PCs, as exemplified by solid digestate samples in both tables [49]. To support this statement, a comparison of SSA for PCs and GCs is shown in Figure S1 (Supplementary Materials). BET SSA in GCs is also influenced by the heating method:

microwave-assisted gasification tends to yield significantly higher SSA than conventional electric heating. The SSA of the GCs also depends on the heating system used. GCs with microwave heating have been shown to exhibit significantly higher SSA compared to those obtained using conventional electric heating [50]. Non-activated GCs listed in Table 3 exhibit SSA BET values ranging from 11 to 1027 m^2/g [49–53]. However, chemical activation significantly enhances their porosity using KOH [54]. Chemically activated chars that use only KOH have also been confirmed to achieve higher surface areas compared to those activated by a hybrid KOH/CO_2 method [55]. Another important parameter that influences SSA is the equivalence ratio (ER), defined as the ratio between the actual amount of air supplied to the gasifier and the amount required for complete combustion. Higher ERs have been shown to result in lower SSA values [56]. Unlike pyrolysis, where increasing temperature can improve SSA, high temperature gasification often reduces microporosity due to increased carbon burn-off and ash accumulation [52]. Therefore, activation is even more critical for GCs to restore and enhance their surface properties.

Detailed analysis of CO_2 adsorption capacities in different chars is provided in Section 3.2.3, where the adsorption capacity is discussed in relation to the activation strategy.

Table 3. Effect of biomass types, temperature (T), atmosphere, residence time (RT) and activation conditions on the specific surface area of GCs.

Biomass Types	Gasification			Activation				BET SSA, m^2/g	Refs.
	T, °C	Atmosphere	RT, min	Method	T, °C	RT, min	C:A [a]		
Solid digestate	600	N_2/Steam	9	Raw	-	-	-	11	[49]
	700							337	
	800							461	
	900							374	
Corn stalk	600	CO_2	25	Raw	-	-	-	452 [b]	[50]
	700							481 [b]	
	800							512 [b]	
	900							526 [b]	
	1000							490 [b]	
	600							312 [c]	
	700							408 [c]	
	800							481 [c]	
	900							503 [c]	
	1000							423 [c]	
Straw	725–750	Air	-	Raw	-	-	-	75 [d]	[51]
Wood								426 [e]	
Wood								1027 [f]	
Wheat straw	800	CO_2	30	Raw	-	-	-	470	[52]
	900							892	
	1000							624	
Hay	800	CO_2	30	Raw	-	-	-	256	[52]
	900							419	
	1000							269	
Poplar wood	750	N_2/Steam	30	Raw	-	-	-	429	[53]
	750	N_2/Steam	60					621	
	750	N_2/CO_2	30					435	
	920	N_2/CO_2	30					687	
Wood chips	900	-	-	Raw	-	-	-	603	[54]
				KOH	600	60	1:1	774	
				$ZnCl_2$	600	60	1:1	739	

Wood	800–1000	Air	180	Raw KOH KOH/CO_2	- 850 850/550	- 120 120/60	- 1:1 1:1/1:100	126 1282 1013	[55]
70% Wood 30% Manure	800–1000	Air	180	Raw KOH KOH/CO_2	- 850 850/550	- 120 120/60	- 1:1 1:1/1:100	256 1409 1404	[55]

[a] C:A is the ratio of gasification char to the activating agent. For activating agents in solid state, this refers to the mass ratio of gasification char to the activating agent. For CO_2 as the activating agent, it refers to the ratio of the mass (in grams) of gasification char to the volume of CO_2 (in cm^3). [b] Microwave gasification. [c] Electric gasification. [d] Particle size 0–0.1 mm, [e] 0–0.5 mm. [f] 0.5–1 mm.

The comparison of Tables 2 and 3 shows that PCs generally offer a wider range of surface areas in their unmodified state and respond more effectively to thermal treatment alone. In contrast, GCs are more dependent on chemical activation to attain similar or superior surface areas. This difference likely stems from the harsher oxidative environment and the higher ash content characteristic of gasification, both of which inhibit the development of natural micropores. Additionally, PCs tend to preserve more oxygenated surface functional groups that contribute to the affinity of CO_2, while GCs are often more aromatized and contain fewer heteroatoms, affecting both the physisorption and chemisorption mechanisms.

In summary, PCs might be more dependent on activation because their original porosity from pyrolysis is not high compared with that of GCs. Ultimately, the choice between PCs and GCs depends on the process parameters, targeted modification strategies, and cost–performance trade-offs.

3.1.2. Pore Size Distribution

The pore size distribution (PSD) in PCs is typically dominated by micropores and mesopores, particularly when material is produced at moderate temperatures (400–500 °C) [57,58]. GCs, on the contrary, tend to exhibit broader pore structures, as micropores coalesce into mesopores and macropores under oxidative and high-temperature conditions [49,59,60]. These structural differences influence the adsorption behavior: micropores are crucial for CO_2 capture due to their size similar to the kinetic diameter of CO_2 molecules, while mesopores and macropores facilitate faster diffusion and improve overall adsorption kinetics. Table 4 shows a comparison between the pore size distribution for the chars produced by pyrolysis and gasification.

Table 4. Comparison of the pore size distributions of pyrolysis and gasification chars.

PC				
Feedstock	**T, °C**	**Dominant Pore Types**	**Main Observations**	**Ref.**
Wheat straw	>350	Macropores (>75 μm)	Larger macropore volumes; suitable for improving soil structure and supporting larger organisms (e.g., nematodes, protists).	[57]
Rice husk	<550	Mesopores (30–75 μm)	Higher mesopore volume; beneficial for increasing plant-available water.	[57]
Miscanthus straw	<350	Micropores (5–30 μm)	More micropores; may serve as habitat for bacteria and fungal hyphae.	[57]
Wheat Straw	500–700	Micropores (44–75%)	Micropores increase with temperature; short residence time at 700 °C yields the highest microporosity (75%). The mesopore content declines and the macropores remain minimal.	[58]
GC				

Poplar Wood	1150	Micropores (constant), mesopores (minor), macropores (vascular channels)	Despite > 90% char conversion, the micropores remain unchanged. Pore volume increases due to vascular channel wall thinning and macropore growth.	[60]
Pine wood	700, 750, 800	Micropores (<2 nm)	Micropores dominate the surface area, but mesopores grow faster initially. Beyond 70% conversion, macropores increase while mesopores decrease, indicating progressive pore widening.	[59]

3.1.3. Ash, Fixed Carbon, and Volatile Matter

The ash content constitutes a relevant factor that influences the overall adsorption efficiency. As highlighted by the arrows in Figure 2a,b, increasing pyrolysis and gasification temperatures are strongly associated with elevated ash content in the resulting chars. It varies widely for both types of char, depending on the feedstock. An increase in pyrolysis temperature leads to a decrease in the content of volatile matter, accompanied by a relative increase in the content of ash resulting from the loss of volatiles [61]. Analyzing the review work [62], GCs ash due to inorganic accumulation under oxidizing conditions ranges from 2% to 75%. However, as illustrated in Figure 2a, the ash content in PCs can reach 74% [63], underscoring the significant influence of the type of feedstock (in this case it was pig manure) on the resulting char composition. The low ash content of PCs provides a better adsorption potential by preserving surface accessibility [64].

The fixed carbon content has also changed with temperature and can range from 3.2 to 92% in PCs, and up to 90% (in GC) under optimized conditions [64,65]. Fixed carbon content increases with pyrolysis temperature, while in the case of gasification, particularly under a steam atmosphere, a decrease has been reported [66]. As shown in Figure 2a,b, PC contains a lower proportion of volatile matter compared to GC.

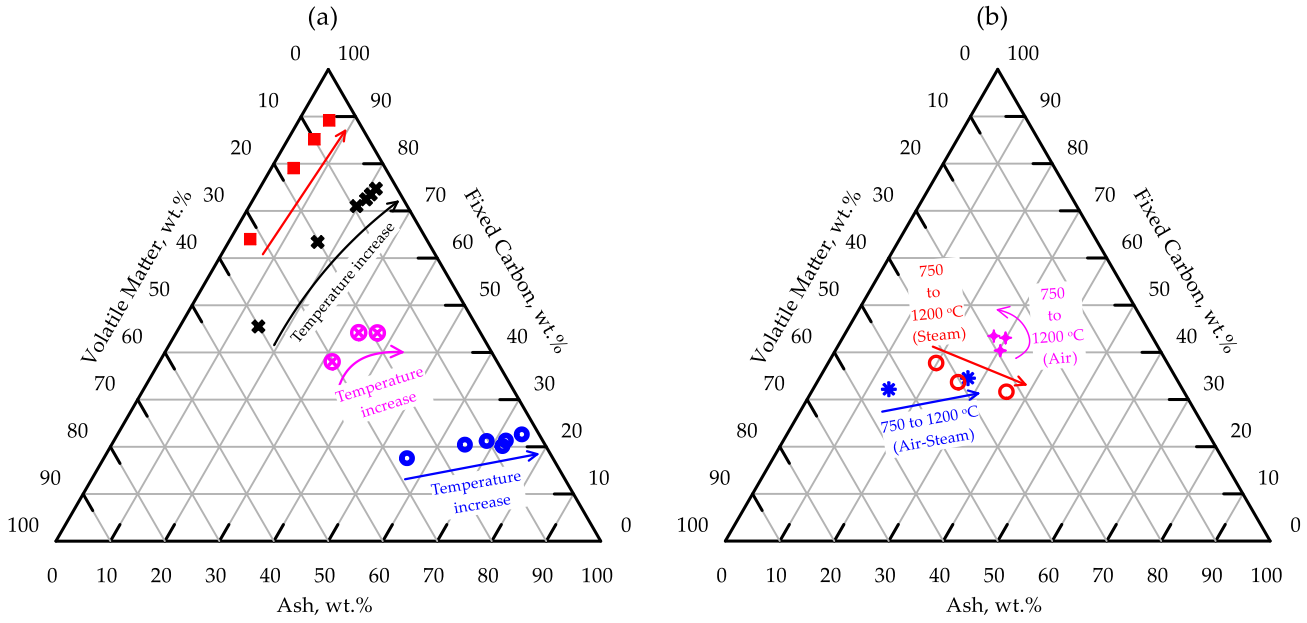

Figure 2. Ash, volatile matter, and fixed carbon contents of non-activated (**a**) PCs and (**b**) GCs (based on the literature data: ■● [63], ✖ [67], ⊗ [68], ✱○✦ [66]).

3.1.4. Hydrogen-to-Carbon and Oxygen-to-Carbon Ratios

The aromaticity of char materials is a critical structural property that influences their thermal stability, chemical reactivity, and performance in CO_2 adsorption applications. The aromaticity of char is commonly assessed using elemental ratios, particularly the hydrogen-to-carbon (H:C) and oxygen-to-carbon (O:C) atomic ratios, which serve as proxies

for structural condensation and oxidation states, respectively. Figure 3a,b illustrate the evolution of these ratios in biomass-derived chars during pyrolysis and gasification. A decreasing H:C ratio reflects increased aromatic condensation and carbonization. As shown in Figure 3a, PCs with H/C < 0.25, typically produced at temperatures above 800 °C, indicate highly condensed aromatic structures with high thermal stability [33,42,49]. On the contrary, higher H:C values suggest the presence of aliphatic groups and lower structural stability [69]. The O:C ratio complements this analysis by indicating the degree of oxidation and polarity; lower values (e.g., <0.2) denote more hydrophobic and aromatic materials. In comparison, GCs tend to retain slightly lower O:C values in similar H/C ratios [49,52,54]. These differences probably arise from variations in reaction atmosphere (inert vs. oxidative), heating rate, and the presence of gasifying agents, which influence devolatilization and aromatic ring formation.

In general, aromaticity and thermal stability increase with process temperature. Pyrolysis promotes the formation of stable polyaromatic ring systems [70]. On the other hand, gasification, which is often carried out under more severe thermal and reactive conditions, can result in even more carbonized and condensed aromatic structures [71]. Petersen and Sanei [72] underscore the robustness of the H:C molar ratio as a key indicator for to evaluate char carbonization, but caution against relying solely on it to evaluate char permanence in carbon sequestration initiatives.

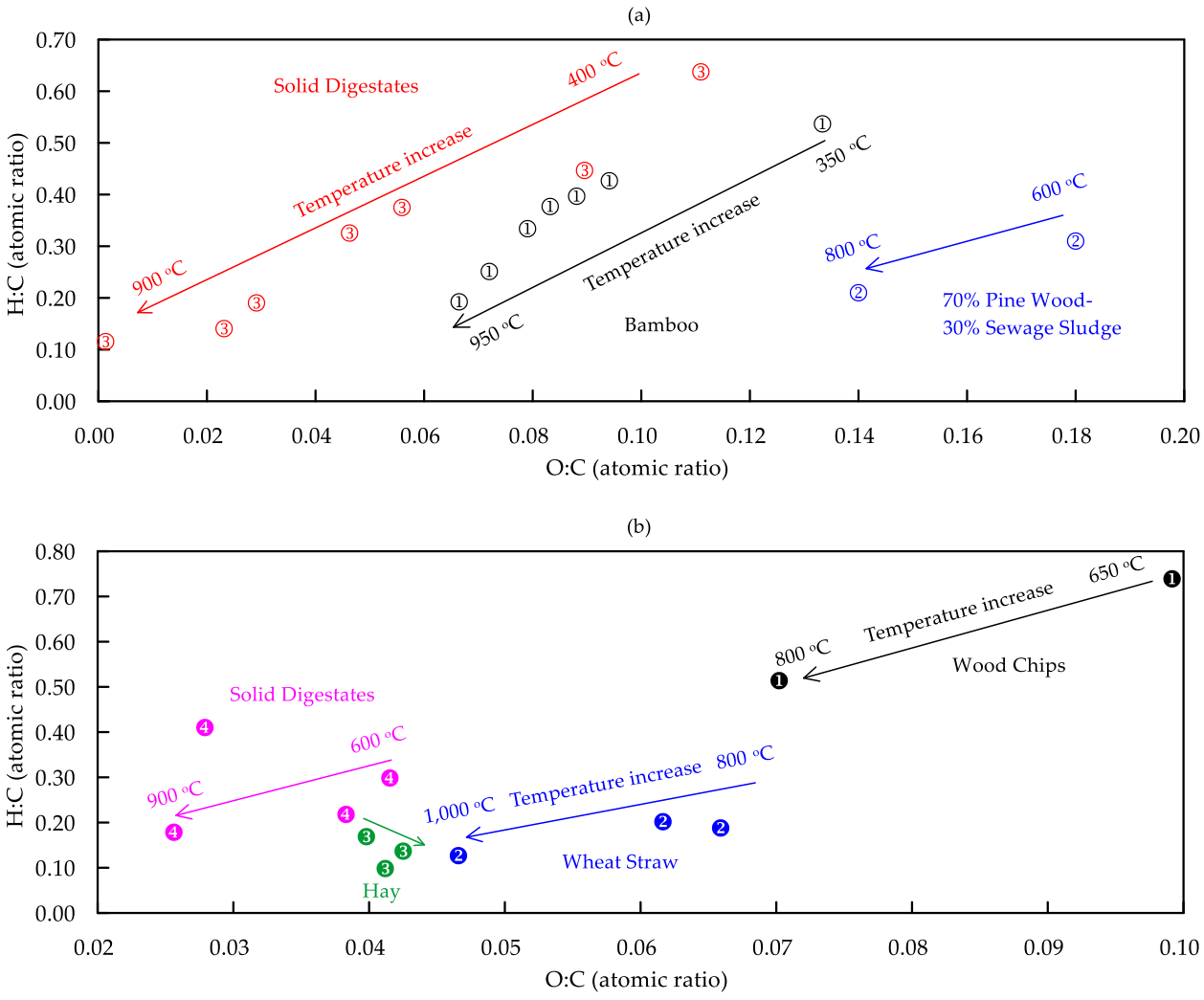

Figure 3. Comparison of H:C and O:C ratios for non-activated chars obtained via (**a**) pyrolysis and (**b**) gasification (Sources: ① [42], ② [33], ③ [49], ❶ [54], ❷ [52], ❸ [52], ❹[49]).

3.2. Adsorption Mechanisms

CO_2 adsorption on char-based materials occurs through a combination of physical and chemical interactions, largely determined by surface functionality and pore structure.

3.2.1. Surface Chemistry

The surface chemistry of the chars significantly affects its CO_2 adsorption capacity, especially under the low partial pressure characteristic of DAC applications. PCs generally retain more oxygenated surface functional groups, including carboxylic, lactonic, phenolic, and quinonic moieties as a function of feedstock type and pyrolysis conditions [73]. The content of surface acidic functional groups decreases significantly with increasing pyrolysis temperature, indicating a transformation from aliphatic to more aromatic structures. In turn, the total surface basicity of PCs increases as the temperature increases, in correlation with the observed elevation in the pH of the char [67]. In contrast, GC contains fewer oxygenated groups due to more intense oxidative processing conditions [74].

3.2.2. Nitrogen Function Groups

Regarding nitrogen-containing functionalities, PC can retain or even enhance these groups, particularly when the feedstock is protein-rich or when doping is applied, thus introducing basic surface sites favorable for CO_2 interaction [75]. GC typically exhibits a very low nitrogen content, as nitrogen species are volatilized during the high-temperature treatment [76].

3.2.3. CO_2 Adsorption Capacity

The capture of CO_2 by PCs and GCs is predominantly governed by two mechanisms: physical adsorption and chemical adsorption (Figure 4). Physical adsorption is based on weak van der Waals forces and is most effective in chars that have well-developed microporous networks and large surface areas, which facilitate the capture of CO_2 within microporous domains [77]. Chemical adsorption, on the other hand, involves more specific and energetically favorable interactions between CO_2 and surface functional groups, including oxygen- and nitrogen-containing moieties (e.g., –OH, –COOH, pyridinic or quaternary nitrogen), that serve as chemisorption-active centers [78]. Moreover, relative to single-heteroatom doping, dual-heteroatom functionalization enhances the density and diversity of CO_2-active sites [79]. Surface modification techniques, including chemical activation (e.g., KOH, H_3PO_4), steam activation, or impregnation with amine compounds (such as polyethyleneimine, PEI), are frequently employed to increase surface area, pore volume, and functional group density, thus improving overall sorption capacity and selectivity toward CO_2.

The CO_2 adsorption capacity of the pyrolysis and gasification chars is typically measured using volumetric or gravimetric techniques, both of which allow for reliable quantification under controlled conditions. The adsorption capacity is strongly influenced by temperature and pressure [54,55]: higher adsorption temperatures tend to reduce CO_2 adsorption capacity due to increased kinetic energy of the gas molecules, whereas increasing pressure generally enhances CO_2 adsorption by promoting greater interaction between the gas and the char surface. To provide a consistent basis for comparison, Table 5 presents a literature-based summary of CO_2 adsorption capacities for various PCs and GCs under standardized conditions of 25 °C and 100 kPa.

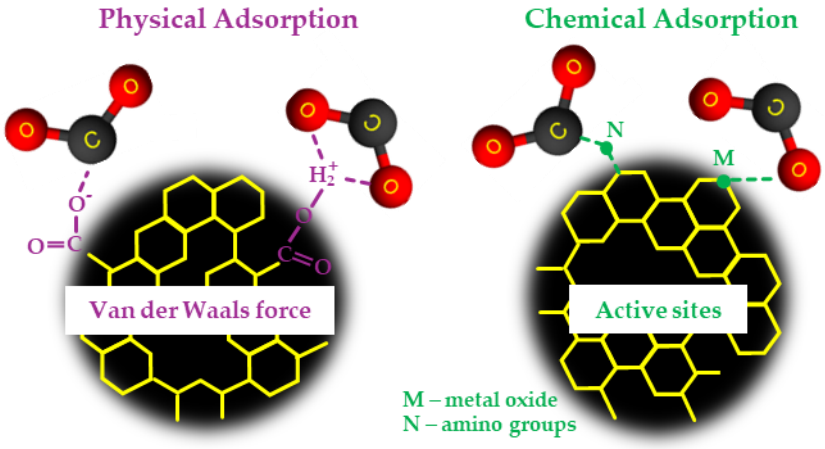

Figure 4. Simplified illustration of CO_2 physisorption and chemisorption mechanisms.

Table 5. Summary of CO_2 adsorption capacities of pyrolysis and gasification chars under different preparation and activation conditions.

PC								
Feedstocks	**Activation**			**Doping element**	**CO_2 Concentration, %**	**CO_2 ads. Capacity in 1st Cycle [(b)], mg/g**	**CO_2 ads. Capacity After 10th Cycle [(b)], mg/g**	**Refs.**
	Methods	**T, °C**	**C:A [(a)]**					
Eucalyptus sawdust	KOH	600; 650; 700; 800 600; 700; 800	1:2 1:2 1:4 1:4	-	100 100 100 100	212; 206; 190; 170 128; 128; 130	-	[32]
70% Pine wood 30% Sewage sludge	Raw	-	-	-	100	43	-	[33]
	KOH	600; 700; 800	1:1	-	100	137; 187; 142	-; 181 138	[33]
Garlic peel	Raw	-	-	-	100	73	-	[43]
	KOH	600; 700; 800 600	1:2 1:2 1:4	-	100 100 100	186; 176; 124 125	-	[43]
Whitewood	Steam CO_2 KOH	700 890 775	1:0.94 1:8.7 1:1.23	-	30 30 30	59 63 78	51 63 77	[44]
Pine sawdust	Steam KOH	850 850	1:0.4 1:3	-	100 100	104 156	-	[45]
Wood pellet	Raw Steam CO_2 $ZnCl_2$ H_3PO_4 KOH	- 550 550 550 550 550	- 1:2.5 1:16.7 1:1 1:1 1:1	-	15 15 15 15 15 15	168 175 175 178 172 180	-	[48]
Coffee grounds	KOH	600	1:2 1:3	-	100 100	132 132	-	[80]
Pomegranate peels	KOH	700	1:1	-	100	181	-	[81]
Carrot peels	KOH	700	1:1	-	100	184		
Fern leaves	KOH	700	1:1	-	100%	181		
Rice husk	CO_2	900	-	-	100	136	-	[82]

Bamboo	KOH	500; 600; 700; 800; 850	1:3	-	100	187; 308; 308; 279; 242	-	[83]
Grass cuttings	CO_2	800	-	-	100	119	-	[84]
Coconut shell	Raw H_3PO_4 KOH	- 600 800	- 1:2 1:4	-	100	60 75 50	-	[85]
Enteromorpha	KOH	700; 800; 900	1:3	-	100	125 [(d)]; 126 [(d)]; 127 [(d)]	-	[86]
Enteromorpha	KOH	700	1:3	N, S [(c)]	100	123 [(d)]; 121 [(d)]; 119 [(d)]	-	[86]
	KOH	800	1:3	N, S [(c)]	100	121 [(d)]; 130 [(d)]; 121 [(c)]		
	KOH	900	1:3	N, S [(c)]	100	122 [(d)]; 121 [(d)]; 120 [(d)]		
Greasyback shrimp shell	KOH	800	1:1 1:2 1:3	N	100	190 157 155	-	[87]
Water chestnut	KOH	600; 650; 700; 800	1:3	N		158; 180; 207; 141		[88]
Coconut shell	KOH	600; 650; 700	1:2 1:3 1:4	N	100	180; 180; 180 176; 211; 207 189; 189; 194	-	[89]
Peanut shell	KOH	680; 730; 780	1:2	N	100	194; 186; 172	-	[90]
Sugarcane bagasse	KOH	500; 600; 700; 800	1:2	N	100	158; 211; 208; 190	-	[91]
Camphor leaves	KOH	500; 600; 700; 800	1:2	N	100	122; 165; 124; 107	-	[92]
				GC				
Wood	Raw KOH KOH/CO_2	- 850 850/550	- 1:1 1:1/1:100	-	100	27 33 37	- - ~37	[55]
70% Wood 30% Manure	Raw KOH KOH/CO_2	- 850 850/550	- 1:1 1:1/1:100	-	100	22 31 29	- - ~29	[55]
Olive stones	Raw	-	-	-	100	106–136 [(e)]	-	[93]
Almond shell	Raw	-	-	-		101–119 [(e)]		
Bagasse	Raw	-	-	-	100	106	106	[94]
Macadamia nut shell	Raw				100	123	123	
Rice straw	Raw				100	53	53	
Palm shell	Raw	-	-	-	100	96	-	[95]

[(a)] C:A is the ratio of char to the activating agent. For activating agents in the solid state, this refers to the mass ratio of char to the activating agent. For CO_2 as activating agent, it refers to the ratio of the char mass (in grams) to CO_2 volume (in cm^3). [(b)] at 25 °C and 100 kPa; [(c)] $Na_2S_2O_3 \cdot 5H_2O$ to PC was set to 0.25:1, 0.5:1, 1:1; [(d)] at 30 °C and 100 kPa; [(e)] lower value for gasification time of 0.5 h and higher for 8 h.

In general, raw PCs show moderate CO_2 adsorption capacities, typically ranging from 43 to 169 mg/g [33,43,48,85], depending on feedstock and production conditions. However, activation, particularly chemical activation using KOH, significantly enhances its capacity, with values that frequently exceed 150 mg/g and reach 308 mg/g for bamboo-

derived char [83]. Similar high-performance levels are observed for KOH-activated eucalyptus [32], garlic peel [43], and sugarcane bagasse [91]. The adsorption capacity tends to increase with activation temperature up to an optimal point, beyond which excessive thermal treatment may reduce the density of functional groups or lead to pore collapse. In addition, doping with heteroatoms such as nitrogen and sulfur has been shown to further improve CO_2 adsorption capacity by increasing the number of basic and chemically active sites on the surface of the char [86–92].

On the contrary, GCs in their raw form tend to exhibit lower CO_2 adsorption capacities, commonly ranging between 22 and 136 mg/g [55,93–95]. This is attributed to their more condensed aromatic structure and lower surface functional group density as a result of harsher gasification conditions. However, GCs also respond positively to chemical activation, and KOH-activated GCs achieve improved capacities of up to 33–37 mg/g under standard conditions [55]. Nevertheless, even after activation, their capacities generally remain below those of comparably activated PCs.

The disparity in adsorption capacity between PCs and GCs is largely attributed to differences in surface chemistry and textural properties. PCs retain more oxygen- and nitrogen-containing groups, which favor chemisorption, while GCs, though often more graphitized, have fewer polar surface functionalities. Additionally, PCs exhibit greater tunability via process parameters, whereas GCs typically require a more aggressive post-treatment to approach a similar adsorption capacity.

These findings suggest that PCs, particularly those subjected to chemical activation and nitrogen doping, are better suited for DAC applications under ambient conditions. However, GCs may still offer viable low-cost options, especially when co-produced in integrated systems or enhanced through advanced activation strategies.

3.2.4. Regeneration Energy, Cyclic Stability, and Environmental Degradation Risks

The viability of DAC systems depends not only on the initial CO_2 adsorption capacity but also on the energy required for regeneration, the durability of the sorbent over repeated cycles and its resistance to environmental degradation. PCs and GCs generally exhibit favorable regeneration profiles due to their physisorption-dominated mechanisms, which involve weak van der Waals interactions and low adsorption heats (~20 kJ/mol), allowing CO_2 to be desorbed with minimal thermal input [32,96]. Experimental results confirm that porous carbons can achieve rapid and nearly complete CO_2 desorption at mild temperatures (e.g., >95% release within 3 min), maintaining capacity over multiple cycles [32,82].

However, some studies report small but progressive decreases in adsorption performance after five or more cycles, attributed to irreversible chemical interactions between surface functional groups (particularly N- and S-doped sites) and CO_2, which can lead to loss of heteroatoms and mass [86]. Despite this, several doped chars retain over 95% of their initial capacity after ten cycles, indicating promising recyclability for DAC applications [86]. Still, long-term data over hundreds or thousands of cycles remain sparse and must be a research priority to validate commercial feasibility [25].

From an energy perspective, the total regeneration demand, including both thermal and electrical components, remains a bottleneck for DAC. PCs and GCs can benefit from electric or hybrid regeneration methods, especially when powered by renewable sources or low-grade waste heat, enhancing their environmental and economic performance [19,25]. Operating conditions such as humidity also affect energy requirements; while humidity has limited impact on adsorption kinetics, it can influence thermal regeneration demands and system design [97].

The risks of environmental degradation, especially due to trace atmospheric contaminants such as ozone (O_3), sulfur oxides (SO_x), and nitrogen oxides (NO_x), present additional concerns. These oxidants can degrade carbonaceous adsorbents by surface oxidation or destruction of active sites, as has been observed in amine-based systems [98,99]. Although PCs and GCs are generally more stable, studies indicate that O_3 can still react with double bonds C=C, especially during desorption heating, leading to material degradation [98]. Moreover, long-term exposure to SO_x and NO_x can shorten the useful life of the sorbent and increase operating costs [99]. Therefore, future testing protocols must incorporate realistic ambient air conditions, including pollutants and co-adsorbed gases, to evaluate the resilience of char-based sorbents under true DAC scenarios.

3.3. Spectroscopic Characterization

Several analytical techniques are commonly used to characterize chars, including Fourier transform infrared spectroscopy, carbon-13 nuclear magnetic resonance spectroscopy, X-ray photoelectron spectroscopy, and Raman spectroscopy.

3.3.1. Fourier Transform Infrared Spectroscopy

Char surfaces are enriched with various functional groups that serve as active sites for CO_2 interactions. The chemical nature of these groups significantly influences the sorption mechanisms and the overall reactivity of the carbonized material. Fourier transform infrared (FT-IR) spectroscopy is widely used for characterizing PCs and GCs, in which the sample absorbs infrared radiation at wavelengths corresponding to the vibrational frequencies of specific chemical bonds. FT-IR spectra provide information on the surface functional groups and chemical structure of the analyzed material [100]. Numerous studies have shown that the temperature of pyrolysis [101,102] and the temperature of gasification [50,103] are a key factor influencing the presence of oxygenated functional groups, which decreases significantly with increasing temperature. Brewer et al. [104] compared FT-IR spectra of PCs (from fast and slow pyrolysis) and GCs. Fast PCs exhibited the highest intensity of oxygen-containing groups (e.g., O–H ≈ 3400 cm^{-1}, C=O ≈ 1700 cm^{-1}), while slow pyrolysis and GCs showed progressively lower functional group signals and stronger aromatic features, with GCs showing only weak peaks below 1800 cm^{-1}. As the pyrolysis temperature increases from 500 to 600 °C, the bands associated with aromatic CH and C=C (observed in the range of 730 to 895 cm^{-1} and 1566 to 1650 cm^{-1}, respectively) and phenolic C–OH (from 1260 to 1310 cm^{-1}) increased significantly [105]. With increasing pyrolysis temperature, the vibrational intensity of the aromatic functional groups decreases, indicating the progressive decomposition of the carbon material and a gradual increase in the character of the formed PC [106]. Similar conclusions were drawn for GC obtained at 900 °C, which exhibited a nearly featureless FT-IR spectrum [107]. This absence of characteristic peaks indicates that most surface functional groups were eliminated during thermal treatment, resulting in an almost purely carbonaceous solid.

Generally, these spectral changes confirm the transition from oxygenated, aliphatic-rich surfaces to more condensed, aromatic carbon matrices. This evolution of surface chemistry has direct implications for CO_2 capture, as the decrease in polar oxygenated groups can reduce chemical affinity, while the formation of microporous aromatic domains improves the physical adsorption capacity.

3.3.2. Carbon-13 Nuclear Magnetic Resonance

Solid-state ^{13}C nuclear magnetic resonance (^{13}C NMR) spectroscopy is a valuable technique for characterizing the structural composition of chars by distinguishing between various carbon environments such as alkyl, O-alkyl, aromatic and carboxylic carbons. It enables the calculation of aromaticity indices based on the relative abundance of

aromatic carbon signals (typically 110–145 ppm), which are indicative of thermal maturity and the potential sorption stability of the material.

Reviewed studies consistently show that increasing the temperature of pyrolysis leads to greater aromaticity, reflected by a higher share of condensed aromatic carbons and a reduction in O-alkyl and aliphatic structures [104,108,109]. The aromaticity values derived from NMR correlate with thermal stability and reduced reactivity, which are critical parameters for long-term CO_2 capture. Among the different pyrolysis modes, slow pyrolysis yields the highest proportion of edge-site aromatic –CH groups, compared to fast pyrolysis and gasification [110]. This is favorable for surface interactions with CO_2. Some studies also highlight the influence of feedstock composition and post-treatment on final aromatic character, suggesting that lignin-rich and manure-derived materials promote stable polyaromatic networks [111,112]. On the contrary, GCs often show more condensed but less protonated aromatic domains, with broader or weaker NMR signals due to increased graphitization and possible interference from residual inorganics [110]. Despite these limitations, NMR remains a robust method for comparing the carbon structure of chars and identifying materials with favorable long-term properties for carbon sequestration.

3.3.3. X-Ray Photoelectron Spectroscopy

X-ray photoelectron spectroscopy (XPS) enables quantitative analysis of surface elements and their chemical states by detecting photoelectrons emitted from a material upon X-ray irradiation. XPS provides quantitative data on the presence of elements such as carbon, oxygen, and nitrogen, as well as insight into their chemical environments. In the context of carbonized materials, XPS can be used to evaluate the aromatic character of chars by detecting the relative abundance of sp^2 hybridized carbon (C=C) associated with aromatic structures versus sp^3 hybridized carbon or oxygen-containing functional groups. This makes XPS a valuable tool for assessing the degree of carbon condensation and surface chemistry evolution during pyrolysis or gasification.

XPS analyses of PCs consistently reveal the progressive aromatization and deoxygenation of PCs with an increase in pyrolysis temperature. For example, Bin Mobarak et al. [113] reported high C 1s peaks in PCs of rubber seed shell assigned to graphitic C–C/C–H, with decreasing oxygenated functionalities as temperature increased. The O 1s spectra supported the predominance of phenolic and carbonyl groups at moderate temperatures, while higher temperature samples lacked hydroxyl signatures, indicating advanced carbonization. Similarly, Zhang et al. [114] documented an increase in the intensity of the C=C (signal sp^2) and a decrease in the aliphatic and oxygenated groups with prolonged heating of the biomass of *Taxodium ascendens*. Yang et al. [115] showed that phosphorus-doped chars undergo significant structural evolution, where π–π satellite peaks and shifting P 2p signals confirmed increased aromaticity and possible lattice incorporation of phosphorus atoms at higher temperatures. Other studies [116,117] further emphasized the dominance of sp^2-hybridized carbon after activation or exposure to volatiles, with the former detecting carbonate peaks after KOH activation and the latter observing progressive removal of oxygen groups and enhancement of aromatic C–C/C=C peaks across the pyrolysis range of 250–550 °C.

In contrast, GCs exhibited surface chemistry shaped by reactive atmospheres and inorganic interactions. Wang et al. [118] identified strong carbonate signals (O 1s ~535 eV) and confirmed the presence of $CaCO_3$ and $MgCO_3$ in chars formed in CO_2 at 900 °C, highlighting the participation of minerals in surface chemistry. Zhu et al. [56] used XPS to show dynamic shifts between the C=O and C–O structures in the chars from the air gasification of poplar sawdust, with oxidative atmospheres that promote the formation of sta-

ble C=O at the expense of the C–O groups. Chen et al. [119] found that the oxidative conditions during gasification enhanced the formation of aromatic C–C bonds via thermal cyclization, whereas the CO_2-enriched atmospheres promoted aromaticity more than the inert conditions. In oxygen-enriched gasification, significant enrichment was observed in sp^2 carbon, KOH activation aiding in heteroatom removal and improving structural order [120]. Lastly, Del Grosso et al. [121] demonstrated that GCs from steam/air processes exhibited high fractions of C–C/C–H functional groups, correlating with enhanced aromatic character and surface stability, whereas increased oxygen content in air-only chars led to higher levels of O=C–O groups, indicating a trade-off between aromaticity and surface polarity.

3.3.4. Raman Spectroscopy

Raman spectroscopy is a non-destructive and highly sensitive analytical technique commonly employed to investigate the structural order of carbonaceous materials, including biomass-derived chars. It is particularly effective for detecting sp^2-hybridized carbon structures and graphitic domains. The primary diagnostic features in the Raman spectra of chars are the D-band (~1350 cm^{-1}), which indicates disordered carbon or defects, and the G-band (≈1580–1600 cm^{-1}), corresponding to the in-plane vibrations of graphitic carbon. The intensity ratio of these bands (I_D/I_G) is a widely used parameter to evaluate the degree of structural disorder and aromatic ring condensation in chars.

In PCs studies [114,122–125], a consistent trend was observed in which increasing the pyrolysis temperature leads to a shift of the D and G-bands, reflecting increased aromatic condensation and a higher degree of order [114,122,124]. The I_D/I_G ratio generally increased with temperature, indicating the formation of larger and more condensed aromatic systems, although at very high temperatures, some studies reported a plateau or even a decrease due to incipient graphitization [114,122]. Moreover, secondary parameters such as I_V/I_G or I_S/I_G were also utilized to describe the valley region and cross-linked structures, respectively (I_V denotes the valley intensity, defined as the minimum signal intensity observed between the D and G bands). For example, chars prepared at 750 °C showed significantly improved I_D/I_G and $I_D/I_{(DR+GL)}$ ratios, indicating the growth of aromatic clusters of 3 to 6 rings [114]. The broad deconvolution of overlapping peaks into multiple sub-bands provided further insight into the evolving polyaromatic networks [125].

GCs presented similar D and G bands but often showed higher I_D/I_G ratios compared to PCs under equivalent or even milder thermal conditions [56,119,120]. This suggests that the oxidative or CO_2-rich atmosphere during gasification promotes structural defects and hinders complete graphitization. Some GCs exhibited high values of I_D/I_G (>2.5), indicating the dominance of disordered and defect-containing aromatic domains [119]. Changes in gasifying agents and equivalence ratios significantly influenced carbon structure, with intermediate ratios favoring greater disorder, while higher temperatures or residence times promoted order [56,126]. The persistence of valley regions and shoulder peaks further indicated the coexistence of amorphous and crystalline carbon structures in these materials.

Overall, Raman spectroscopy confirms that both pyrolysis and gasification processes significantly influence the aromaticity and structural evolution of chars. While pyrolysis tends to produce more ordered and thermally stable structures at higher temperatures, GCs often retain a higher level of disorder due to process-specific factors such as partial oxidation and gas–solid interactions.

4. Optimization Strategies and Char-Based Adsorbents

4.1. Structural and Chemical Modifications

Optimization of char physicochemical properties constitutes a fundamental axis to improve its CO_2 adsorption capacity, thereby reinforcing its applicability as an economically viable and environmentally sustainable sorbent for carbon capture systems [127,128]. The adsorption of CO_2 on the char surfaces is governed by a complex interplay between the textural attributes and chemical functionalities of the surface, both of which determine the strength, capacity and selectivity of the adsorption process.

The development of a hierarchical porous architecture within the char matrix is imperative to balance adsorption capacity and mass transfer efficiency. Micropores (<2 nm), particularly those in the range of 0.5–1.0 nm, play a critical role in CO_2 physisorption due to their capacity to induce overlapping potential fields that enhance the strength of van der Waals interactions [129–132]. The confinement of CO_2 within ultramicropores (<0.7 nm) increases the adsorption potential via the Dubinin–Radushkevich mechanism, which is particularly effective at low pressures typical of post-combustion CO_2 capture scenarios [133,134].

However, an excessive development of microporosity can lead to diffusional limitations, particularly at industrially relevant flow rates, due to the restricted mobility of gas molecules within the narrow pore channels [135]. Therefore, the incorporation of mesopores (2–50 nm) serves as transport pathways that alleviate resistances to mass transfer, facilitate faster adsorption kinetics and improve the overall efficiency of the process [136–138]. This dual-pore strategy exemplifies a fundamental design trade-off: optimizing the microporous volume for maximal adsorption while ensuring sufficient mesoporosity for rapid diffusion and facile regeneration.

Beyond textural optimization, the surface chemistry of char exerts a decisive influence on CO_2 adsorption through the introduction of specific functional groups capable of engaging in physicochemical interactions with CO_2 molecules. Oxygen-containing functional groups, such as hydroxyl (-OH), carbonyl (C=O), carboxyl (-COOH), and lactone moieties, can act as weak Lewis base sites that engage in dipole-quadrupole interactions with the quadrupolar CO_2 molecule [139]. However, their contribution is generally limited to enhancement of physisorption through increased surface polarity and hydrophilicity.

However, while nitrogen doping enhances chemisorption strength and CO_2 uptake, particularly under diluted CO_2 conditions as in DAC, it simultaneously introduces a trade-off in terms of regeneration energy. Stronger chemisorption bonds, though beneficial for capture capacity, require greater energy input to reverse during the desorption step, which is intrinsic to cyclic adsorption processes. This leads to an elevated energy penalty during thermal or pressure-swing regeneration, thereby impacting overall process efficiency and operating costs. To address this, recent studies have focused on tuning the type and distribution of nitrogen functionalities to favor moderately strong but reversible interactions, e.g., by maximizing pyrrolic-N over quaternary-N groups, thereby maintaining a balance between capture efficiency and regenerability [140]. Additionally, hybrid adsorbents combining N-doped char with materials exhibiting low regeneration enthalpies (e.g., physisorptive supports or functional coatings) have shown promise in reducing the total regeneration load without compromising CO_2 uptake.

The pyrolysis temperature and residence time profoundly affect the structural order and chemical reactivity of char. Higher pyrolysis temperatures (>800 °C) typically promote the development of graphitic domains through progressive aromatization and dehydrogenation, leading to increased structural ordering of carbon [141,142]. This transfor-

mation improves the mechanical stability and electrical conductivity of char, but concomitantly reduces the density of surface functional groups due to thermal degradation of the oxygen and nitrogen labile moieties [143].

Conversely, lower pyrolysis temperatures (400–600 °C) preserve a greater abundance of reactive functional groups, enhancing surface reactivity and chemisorption potential, although at the cost of reduced thermal stability and mechanical integrity. This requires careful optimization of pyrolysis parameters to achieve an optimal compromise between surface reactivity—crucial for CO_2 capture—and structural robustness, particularly for industrial applications requiring multiple adsorption-desorption cycles. The aromaticity of the carbon structure also modulates π-electron interactions with CO_2. While the CO_2 molecule is linear and nonpolar overall, its quadrupolar nature allows for weak π–π interactions with graphitic domains on the char surface, although these are generally considered secondary to the dominant physisorption and chemisorption mechanisms [144,145].

Contemporary advances in activation methodologies have enabled the fine-tuning of char porosity and surface chemistry to maximize CO_2 adsorption capacity. Physical activation, which typically employs steam or CO_2 as activating agents at elevated temperatures (≈800–1000 °C), facilitates selective gasification of amorphous carbon regions, thus generating additional porosity while preserving the inherent structural integrity of char [146,147].

Chemical activation, using reagents such as potassium hydroxide (KOH), zinc chloride ($ZnCl_2$), or phosphoric acid (H_3PO_4), promotes the development of a highly porous network through complex thermochemical reactions. For example, KOH activation proceeds via the intercalation of K species in the carbon lattice, followed by redox reactions that etch micropores and develop a high surface area structure [148]. Despite its remarkable effectiveness in enhancing microporosity and surface area, the industrial-scale application of KOH activation is considerably constrained by several significant drawbacks. The highly corrosive nature of KOH requires specialized, corrosion-resistant equipment, which increases capital expenditure. Moreover, the cost of KOH and the large volumes needed for activation impose economic burdens. The process also results in high water consumption and generates large amounts of alkaline wastewater during post-activation washing steps, which pose serious environmental challenges and require expensive effluent treatment systems, compromising the environmental viability and scalability of this method [149,150].

To overcome these issues, the concept of "green activation" has emerged as a promising alternative aimed at developing sustainable and environmentally benign activation processes without sacrificing adsorption performance. Green activation approaches include the utilization of bio-derived alkalis, such as potassium salts recovered from biomass ashes, which offer a circular economy perspective by valorizing waste materials. In addition, naturally occurring organic acids such as citric acid can serve as mild activating agents, reducing the environmental impact. Deep eutectic solvents (DES), composed of biodegradable and non-toxic constituents, have also shown potential as effective pore-forming agents. Nevertheless, although lab-scale results are encouraging, more pilot-scale validation is required to confirm their performance, scalability, and long-term environmental safety under industrial conditions [151].

Furthermore, molten salt activation employing low-melting inorganic salts (e.g., NaCl-KCl eutectic mixtures) has gained traction for its ability to produce highly porous carbons under milder conditions, while enabling facile salt recovery and recycling, thereby enhancing process sustainability. Complementing chemical methods, physical activation techniques, such as microwave-assisted activation, offer notable advantages. This method uses volumetric and selective heating of carbon precursors to rapidly induce pore

formation with lower energy consumption and reduced processing time compared to conventional thermal activation methods. However, gains in energy efficiency must be balanced against limitations in heating uniformity and scale-up feasibility, which remain technical hurdles to industrial deployment [152,153]. Collectively, these emerging activation strategies present complementary benefits, but also reveal scalability gaps that must be addressed through techno-economic analyses and pilot-scale demonstrations to ensure their industrial viability.

The advent of computational tools, particularly machine learning (ML) algorithms coupled with molecular simulation techniques, represents a transformative development in the rational design of char-based adsorbents [154]. Data-driven approaches enable the prediction of optimal char properties, such as specific surface area, pore size distribution, and functional group density, based on precursor characteristics and process parameters [155]. For example, density functional theory (DFT) calculations and grand canonical Monte Carlo (GCMC) simulations facilitate the elucidation of adsorption energetics and pore-filling mechanisms at the atomic scale, providing insights that inform experimental synthesis strategies [156,157].

ML models trained on large datasets that encompass diverse char materials and processing conditions have demonstrated the capacity to identify non-obvious correlations and optimize synthesis parameters to achieve target adsorption capacities with minimal empirical experimentation [158,159]. This integration of computational and experimental methodologies accelerates the development cycle of advanced char materials, promoting process intensification, and reducing resource consumption.

4.2. Influence of Pyrolysis Atmosphere on CO_2 Capture Efficiency

The pyrolysis atmosphere constitutes a decisive extrinsic factor that governs not only the thermal decomposition pathways of the precursor material, but also the chemical functionalities and defect structures imprinted onto the resultant char, which, in turn, critically modulate its CO_2 capture performance [160]. This influence operates at both the thermodynamic and kinetic levels, affecting reaction equilibria and promoting distinct reaction mechanisms that govern the physicochemical evolution of the solid carbon matrix.

Under inert atmospheres, such as N_2 or Ar, pyrolysis proceeds predominantly through devolatilization and polycondensation reactions, leading to progressive aromatization and the formation of graphitic domains with relatively low defect densities [161,162]. However, when pyrolysis occurs in reactive atmospheres, additional heterogeneous gas-solid reactions come into play.

For example, under a CO_2 atmosphere, the Boudouard reaction (Equation (5)) is activated at temperatures typically above 700 °C, promoting controlled gasification of the carbon structure.

$$C_{(s)} + CO_{2(g)} \rightarrow 2CO_{(g)};\ \Delta H^\circ = +172.5\ \text{kJ/mol} \quad (5)$$

This reaction not only damages the carbon surface, thereby introducing additional porosity, but also generates active sites such as carbonyl (>C=O) and lactone groups at the pore edges [163–165]. These oxygenated functionalities can serve as basic Lewis sites, promoting specific interactions with the quadrupolar CO_2 molecule through dipole-quadrupole or acid-base mechanisms [166,167].

Similarly, the presence of steam during pyrolysis activates the water-gas shift reaction (Equation (6)) and the water-gas reaction (Equation (7)), which contribute to both porosity development and the incorporation of hydroxyl (–OH) and carbonyl groups on the carbon surface [168,169]

$$C_{(s)} + H_2O_{(g)} \rightarrow CO_{(g)} + H_{2(g)};\ \Delta H^\circ = +131.3\ \text{kJ/mol} \quad (6)$$

$$CO_{(g)} + H_2O_{(g)} \rightleftharpoons CO_{2(g)} + H_{2(g)};\ \Delta H^\circ = -41.1\ \text{kJ/mol} \quad (7)$$

Unlike conventional ex situ activation processes, these in situ gasification reactions proceed concurrently with pyrolytic decomposition, allowing for the simultaneous tailoring of textural and chemical properties without necessitating additional post-treatment steps.

Beyond porosity, the pyrolysis atmosphere exerts a profound impact on surface chemistry by dictating the nature and abundance of surface functional groups that influence CO_2 adsorption through chemisorption mechanisms.

Oxidative or semi-oxidative atmospheres (e.g., limited O_2 or air) promote partial oxidation of the carbon framework, leading to the formation of oxygenated moieties such as carboxylic acids (–COOH), phenolic (–OH), lactones, and quinones [170–172]. These groups increase the surface polarity and allow specific acid-base interactions with CO_2, which is a weak Lewis acid. Notably, carboxyl and hydroxyl functionalities can engage in hydrogen bonding with CO_2, stabilizing its adsorption through reversible complexation mechanisms [77].

On the other hand, pyrolysis under reduced atmospheres, particularly those containing ammonia (NH_3) or urea-derived vapors, promotes nitrogen doping through the incorporation of pyridinic-N, pyrrolic-N, and quaternary-N species into the carbon lattice [173]. Pyridinic-N and pyrrolic-N, located at the edges and defects of graphene layers, are known to enhance CO_2 adsorption through increased local basicity and the ability to donate electron density to the electrophilic carbon atom of CO_2, thus stabilizing its adsorption through Lewis acid-base interactions [78,174]. Furthermore, the presence of quaternary-N improves the electrical conductivity of the material, which may be beneficial for electrochemically assisted CO_2 capture applications.

The interplay between the pyrolysis temperature and the atmospheric composition further complicates the evolution of surface functionalities. At elevated temperatures (>800 °C), most oxygenated groups are thermally unstable and tend to decompose via decarboxylation, dehydration, or decarbonylation reactions, leading to a more hydrophobic and less functionalized surface under inert atmospheres [73]. However, the presence of reactive gases such as CO_2 or steam can mitigate this loss by enabling continuous functionalization through dynamic surface oxidation processes [175]. This duality allows for the generation of thermally stable oxygen functionalities, such as carbonyls and ethers, even at high pyrolysis temperatures.

Moreover, under ammonia-rich atmospheres, nitrogen functionalities can be stabilized at high temperatures through nitridation reactions, leading to the incorporation of graphitic-N species that are more resilient to thermal degradation [176,177]. This stabilization is critical for the long-term performance of nitrogen-doped chars in CO_2 capture applications, particularly under fluctuating operational conditions.

From a process engineering point of view, the deliberate manipulation of the pyrolysis atmosphere offers significant opportunities for the integration of pyrolysis with carbon activation processes, enabling one-step synthesis of highly functionalized chars suitable for CO_2 capture [178,179]. The use of CO_2 or steam as the reactive gas not only valorizes these industrial by-products, but also aligns with the principles of the circular carbon economy by reintegrating captured CO_2 into the production cycle, thereby reducing the overall carbon footprint [180]. However, the selection of atmosphere must also account for operational constraints, such as gas purity, reaction kinetics, equipment corrosion, and safety considerations, particularly when handling reactive or toxic gases such as NH_3 [181].

In summary, modulation of the pyrolysis atmosphere emerges as a strategic lever for the rational design of char materials with optimized surface chemistry and textural properties for enhanced CO_2 capture performance. Future research should focus on elucidating the reaction mechanisms at the molecular level through in situ characterization techniques (e.g., in situ FTIR, XPS under reactive atmospheres), as well as the kinetic modeling of coupled pyrolysis and gasification processes under varying atmospheric compositions [182]. Additionally, the development of scalable pyrolysis reactors with precise atmosphere and temperature control will be essential to bridge the gap between laboratory-scale studies and industrial carbon capture and utilization (CCU) applications [183].

4.3. Coupling Pyrolysis/Gasification with Carbon Capture and Utilization

The integration of pyrolysis and gasification processes with carbon capture and utilization (CCU) frameworks constitutes a burgeoning and promising paradigm for the valorization of carbonaceous residues, especially within the ambit of sustainable energy production and circular carbon management strategies. By synergistically coupling thermochemical conversion with either in or ex situ CO_2 capture and downstream utilization pathways, it is feasible not only to enhance the overall energetic efficiency of biomass or waste conversion, but also to significantly mitigate greenhouse gas emissions through effective carbon recycling [184–186].

Pyrolysis and gasification are intrinsically complementary thermochemical processes. Pyrolysis, typically operated at intermediate temperatures ranging from 400 to 700 °C, facilitates the thermal decomposition of complex organic feedstocks predominantly through bond cleavage reactions such as dehydration, decarboxylation, and depolymerization. This process yields a carbon-rich solid residue—char—characterized by an increasingly aromatic and graphitic microstructure that exhibits an abundance of surface functional groups, including carboxyl, hydroxyl, phenolic and lactonic moieties [187]. These surface oxygenated functionalities confer polar characteristics that enhance the physical adsorption of CO_2 molecules through dipole-quadrupole interactions and hydrogen bonding. Moreover, the presence of heteroatoms and defects within the carbon matrix can facilitate chemisorption mechanisms, particularly acid-base interactions, in which CO_2, a weak Lewis acid, interacts with electron-rich basic sites on the char surface [78,188].

On the contrary, gasification operates at significantly higher temperatures (800–1200 °C) under a controlled supply of oxidizing agents such as O_2, air, steam, or CO_2 itself, thus affecting partial oxidation of the feedstock. This results in the generation of a syngas predominantly composed of CO, H_2, and CO_2, formed through a network of endothermic and exothermic reactions, including the Boudouard reaction (5), the water-gas shift reaction (6), and methanation pathways under specific conditions [189]. In particular, the CO_2 generated within the gasifier can serve as an intrinsic activating agent for the residual char. The high-temperature interaction between CO_2 and carbon leads to a self-activation mechanism whereby CO_2 gasification selectively gasifies amorphous carbon fractions, promoting the development of microporosity and enhancing the specific surface area of the char [190]. This effect improves the adsorptive capacity and regenerability of the char material for subsequent CO_2 capture, thus creating an elegant feedback loop that contributes to carbon recycling within the system.

This coupling strategy realizes a dual benefit: (i) the production of tailored, functionalized chars exhibiting optimized pore size distribution and surface chemistry conducive to selective CO_2 adsorption; and (ii) the generation of a reactive syngas stream that can be either directly utilized as a fuel or feedstock or subjected to advanced separation techniques to isolate and valorize CO_2 [191]. Furthermore, the selective capture of CO_2 from

syngas streams using these optimized chars paves the way for integrated process intensification, wherein adsorbents are derived from the same feedstock conversion process, reducing external material inputs and enhancing overall system sustainability.

The subsequent valorization of the captured CO_2 through CCU technologies encompasses catalytic hydrogenation routes such as methanation (Equation (8)) or methanol synthesis (Equation (9)), mineral carbonation by reaction with alkaline earth metal oxides (Equation (10)), and biological conversions using autotrophic microorganisms [192].

$$CO_{2(g)} + H_{2(g)} \rightarrow CH_{4(g)} + 2H_2O_{(g)};\ \Delta H^\circ = -164.9\ \text{kJ/mol} \quad (8)$$

$$CO_{(g)} + 3H_{2(g)} \rightarrow CH_3OH_{(g)} + H_2O_{(g)};\ \Delta H^\circ = -49.5\ \text{kJ/mol} \quad (9)$$

$$CaO_{(s)} + CO_{2(g)} \rightarrow CaCO_{3(s)};\ \Delta H^\circ = -178.0\ \text{kJ/mol} \quad (10)$$

These pathways enable the conversion of CO_2 into value-added chemicals or fuels, thus transforming the traditionally linear carbon flows of pyrolysis and gasification into closed-loop systems with substantially reduced net carbon emissions. Importantly, the co-production of syngas and high-performance char-based adsorbents aligns with the principles of process intensification and circular economy, maximizing resource efficiency while minimizing waste and environmental impacts.

From a process engineering perspective, the realization of coupled pyrolysis/gasification-CCU systems demands meticulous control over critical reaction parameters, including temperature gradients, residence times, oxidant partial pressures, and feedstock characteristics, to optimize the yield and physicochemical properties of both gaseous and solid products [193,194]. Advances in reactor configurations, such as dual fluidized bed reactors that allow separate pyrolysis and gasification zones, or modular units that integrate sequential thermochemical stages, are essential to ensure seamless coupling with CO_2 capture and utilization modules. Moreover, the durability and cyclic stability of char-based adsorbents under repeated adsorption-desorption regimes remain key operational challenges requiring further material innovation.

Life cycle assessment (LCA) and techno-economic analysis (TEA) studies have underscored the potential of these integrated systems to achieve negative carbon emissions, particularly when deploying lignocellulosic biomass as feedstocks. However, obstacles related to scale-up, system complexity, energy integration, and cost-effectiveness persist, necessitating continued multidisciplinary research efforts to overcome kinetic constraints and ensure the robustness and economic viability of full-scale implementations.

4.4. Integration of CO_2 Recycling in Gasification Processes

The strategic integration of CO_2 recycling within gasification processes represents a key step towards the development of carbon-neutral and potentially carbon-negative thermochemical conversion technologies. By reinjecting either captured CO_2 or internally generated process CO_2 at selective stages of the gasification operation, it becomes possible to manipulate reaction equilibria, improve syngas composition, and foster a more sustainable and circular management of carbon fluxes within the system [195,196].

A principal approach to CO_2 recycling in gasification is its use as a reactive gasifying agent, partially or wholly substituting conventional oxidants such as steam or oxygen. The central reaction involved is the Boudouard reaction (5), a key heterogeneous equilibrium process that occurs at the interface of solid carbonaceous residues (char) and gaseous CO_2 [197–199]. This reaction is fundamentally endothermic, favoring higher temperatures typically above 900 °C, where the equilibrium shifts toward CO production, thereby augmenting syngas yield through efficient conversion of residual char carbon into carbon monoxide [200]. The enhancement of CO concentration in syngas not only improves its

heating value and reactivity, but also enables downstream catalytic syntheses, such as Fischer–Tropsch or methanol production, extending the carbon utilization cascade [201,202].

Beyond the primary role of CO_2 as a gasifying agent, its reintegration offers ancillary benefits that influence both operational economics and process sustainability. By reducing the dependence on external oxidants, especially oxygen, CO_2 recycling decreases costs related to oxygen production and handling, mitigating safety concerns inherent in oxygen enrichment systems [203,204]. Moreover, the valorization of captured CO_2 streams derived from syngas purification units, flue gas post-combustion capture, or industrial point sources fosters closed-loop carbon management, aligning with circular economy objectives and enabling integration with carbon capture and utilization (CCU) infrastructures [205].

On the physicochemical front, CO_2-mediated gasification exerts profound effects on the microstructure and surface chemistry of the residual chars and ash components. The gasification of char by CO_2 promotes selective gasification of less ordered, amorphous carbon phases, leading to enhanced development of microporosity and mesoporosity through carbon gasification etching [206]. This in situ activation modifies the pore size distribution and increases the specific surface area, which can enhance the subsequent adsorption capacity of char for CO_2 or other gaseous contaminants in downstream environmental applications [207,208]. Such self-activation mechanisms mirror those observed under pyrolysis atmosphere modulation, but operate at higher temperature regimes characteristic of gasification.

Despite its advantages, the practical implementation of CO_2 recycling in gasification is limited by intrinsic thermodynamic and kinetic factors. The Boudouard reaction's equilibrium and rate depend sensitively on temperature, pressure, and char reactivity, necessitating tight control of reactor conditions to maximize conversion efficiency and syngas quality [209,210]. Additionally, potential operational challenges include carbon deposition phenomena (coking), catalyst poisoning or deactivation, and tar formation, all of which may impair gasifier stability and longevity. To address these issues, advanced reactor configurations such as dual fluidized bed systems, plasma-assisted gasification, and staged gasifier designs have been developed to enable more effective control over reaction environments and facilitate continuous CO_2 recycling [211].

From a systemic viewpoint, integrating CO_2 recycling into gasification enhances the synergy between thermochemical conversion and broader CCU frameworks. The CO generated through the Boudouard reaction can be channeled into catalytic conversion processes, including Fischer–Tropsch synthesis or hydroformylation, to produce liquid hydrocarbons, oxygenates, or specialty chemicals, valorizing carbon streams and reinforcing economic feasibility. Moreover, integration with renewable hydrogen sources can facilitate further upgrading of syngas components, enabling sustainable pathways for the production of synthetic fuels [212,213].

Finally, comprehensive life cycle assessment (LCA) analyses substantiate the environmental merits of CO_2 recycling integration within gasification. These assessments consistently demonstrate significant reductions in net CO_2 emissions compared to conventional fossil-based thermochemical processes. When biomass or biogenic waste feedstocks serve as carbon sources, these integrated gasification-CO_2 recycling systems exhibit the potential for net negative carbon footprints, contributing meaningfully to climate change mitigation and fulfilling policy mandates for decarbonization [214,215].

4.5. Technological Advances in Char Modification and Activation

Recent technological progress in the modification and activation of char has considerably expanded its capabilities as a highly efficient and selective adsorbent for CO_2 capture, while simultaneously enabling its integration into a wider spectrum of energy conversion and environmental remediation applications. These advances transcend traditional physical activation methods and encompass innovative approaches rooted in materials engineering, surface chemical functionalization, and process intensification strategies [216,217].

Chemical activation remains a cornerstone for tailoring the porosity of the char and surface chemistry. Conventional activating agents such as potassium hydroxide (KOH), phosphoric acid (H_3PO_4), and zinc chloride ($ZnCl_2$) are well-known for their capacity to induce extensive microporosity and mesoporosity through controlled chemical etching and dehydration reactions [218]. These agents interact with the carbonaceous matrix, promoting bond cleavage and volatilization of non-carbon elements, which results in the enlargement of pore volume and development of hierarchical pore networks [219]. For example, KOH activation involves complex redox reactions in which KOH penetrates the carbon matrix, reacts with carbon to form potassium compounds, and releases gases such as H_2 and CO that generate micropores [220].

However, the large-scale application of KOH raises significant concerns related to its environmental impact and economic feasibility. The process requires substantial amounts of KOH and large volumes of water for subsequent neutralization and washing, leading to high operational costs and the generation of alkaline wastewater that requires proper treatment and disposal. These issues limit the scalability and sustainability of KOH-based activation methods, especially when targeting industrial carbon capture processes.

In response to these limitations, the concept of "green activation" has gained traction. It encompasses the development and adoption of environmentally benign alternatives that maintain or improve activation efficiency while reducing ecological burdens. Green activators include biomass-derived alkalis, organic acids, and deep eutectic solvents (DES), which are less corrosive and are easier to recover. Molten salts, such as carbonates or chlorides, have also emerged as effective activating media, enabling high porosity development without generating hazardous residues. In addition, physical methods such as microwave-assisted activation and CO_2 or steam treatment offer cleaner pathways by avoiding chemical residues altogether, making them attractive from both environmental and regulatory perspectives.

Among these, microwave-assisted activation stands out because of its rapid volumetric heating, which enhances energy efficiency and allows for precise control over pore development. Likewise, supercritical CO_2 treatment provides mild-temperature activation that minimizes carbon loss and structural collapse, while maintaining high pore connectivity and adsorption capacity [221].

Beyond pore generation, functionalization of char surfaces has evolved as a crucial strategy to improve CO_2 affinity and selectivity. Incorporation of nitrogen-containing functional groups, through techniques such as post-synthetic amination or co-pyrolysis with nitrogen-rich precursors (e.g., urea, melamine), introduces basic sites that enhance acid-base interactions with acidic CO_2 molecules [222]. The basic nitrogen moieties, including pyridinic, pyrrolic, and quaternary nitrogen, contribute electron lone pairs that interact with the CO_2 quadrupole moment via dipole-quadrupole forces and Lewis acid-base interactions, thereby increasing adsorption capacity and selectivity [223,224]. Similarly, grafting metal oxides (e.g., MgO, CaO) or nanoparticles onto the char surface facilitates chemisorption mechanisms and may provide catalytic sites that enable CO_2 activation and conversion reactions [78,225]. These hybrid materials exhibit multifunctionality, combining adsorption with catalytic transformation capabilities.

In parallel to chemical methods, advanced physical activation approaches have gained significant attention. Techniques such as supercritical CO_2 treatment allow pore development under mild temperature conditions, minimizing structural damage while improving pore connectivity and volume [226,227]. Steam activation under controlled atmospheres is also utilized to create oxygen-containing surface groups that enhance hydrophilicity and CO_2 binding sites without excessive burn-off of carbon. Microwave-assisted pyrolysis represents a particularly promising technology due to its rapid and volumetric heating, which promotes uniform activation and reduces processing time [228]. The rapid heating rates facilitate the formation of hierarchical pore structures that improve multi-scale mass transfer, a critical feature for practical adsorption systems.

At the nanoscale, templating methods—both hard (e.g., silica, alumina) and soft (e.g., block copolymers, surfactants)—have revolutionized the synthesis of ordered porous carbons with highly uniform pore size distributions and tailored geometries optimized for CO_2 diffusion and adsorption kinetics [229]. Hard templating exploits sacrificial inorganic templates to produce carbons with a precise mesopore architecture upon template removal. Soft templating provides more flexible and scalable routes, enabling the formation of mesoporous and microporous carbons with tunable morphology under mild synthesis conditions.

The integration of these chemical, physical, and templating techniques has led to the development of multifunctional chars suitable for dynamic adsorption processes such as temperature swing adsorption (TSA) and pressure swing adsorption (PSA) systems. These materials exhibit enhanced CO_2 adsorption capacity, superior regeneration stability, and mechanical robustness, critical for the cyclic loading and unloading conditions encountered in industrial carbon capture applications [230,231].

Complementing experimental advancements and computational materials science tools have become instrumental in the rational design of char-based adsorbents. Density functional theory (DFT) and molecular dynamics (MD) simulations enable atomic-scale understanding and prediction of adsorption energetics, pore size effects, and functional group interactions with CO_2 [232]. Such simulations reduce the reliance on empirical optimization, guiding the targeted synthesis of char materials with optimized pore structures and surface chemistries, thus accelerating the development of next-generation CO_2 adsorbents with tailored performance metrics.

5. Key Challenges and Limitations

This section highlights the urgent need to look for innovative procedures to reduce atmospheric CO_2 levels, as well as minimize gaseous emissions from various emission sources. In this context, several researchers around the world present perspectives and key challenges, as well as possible limitations to the implementation of these strategies.

In a recent review, Wu et al. [3] listed that a major challenge for the implementation of DAC can be understood in the integration of new component technologies through the implementation of large-scale commercial projects. Such an application can go beyond the energy sectors, as well as the various industrial sectors that emit CO_2, such as the metallurgical, steel, and civil construction industries, which are not easy to decarbonize.

For Liu et al. [11], studies that evaluate DAC are extremely important and bring interesting challenges even in low concentration atmospheres. The authors also stated that these studies open new perspectives for treating some municipal waste (sewage sludge char), as they demonstrate its use and utilization in a rational way, making it possible to treat waste with waste, extracting its potential, and presenting incomparable social and environmental benefits.

In the review article, Faizan and Song [37] highlighted the formation of tar in gasifiers during the continuous gasification of the lignocellulosic substrate as one of the main problems for commercialization. The authors focused on recent advances in biomass gasification using various techniques, for example supercritical water, catalytic steam gasification and catalytic CO_2 gasification, and discussed improvements in gasification process, parametric impacts, biomass pretreatments, and catalytic deactivation mechanisms to overcome challenges, limitations, and improve catalytic yield. The future direction and critical perspectives of catalytic biomass gasification were also analyzed, which considered and highlighted socio-environmental and economic aspects as depreciating factors.

Sabatino et al. [233] conducted a comparative study on the cost assessment and optimization of energy consumption for the implementation of DAC technologies. Some parameters such as productivity, exergy analysis, and energy consumption were calculated, based on process simulations and mathematical optimization. The authors discussed the necessary costs, challenges, and limitations for the implementation of DAC systems on a large scale. They showed that all the technologies employed provided CO_2 with high purity and good performance, but required high exergy and productivity. As a limitation, they showed that productivity and energy consumption for CO_2 capture, within a large-scale system, is a high capital cost, which is a very determining factor.

According to Realmonte et al. [234], the urgency of large-scale atmospheric CO_2 removal to achieve the most stringent global climate goals remains unmet. The authors presented some mechanisms for DAC using char, which are considered innovative alternative options for mitigating these emissions. They conducted a first comparison on the role of DAC in some temperature variation scenarios, under technical-economic circumstances. They reported that the implementation of DAC using char significantly reduces and complements mitigation costs, possibly not requiring replacement by other NET forms, bringing great potential for the implementation of this type of system. However, they also warned that a limiting factor for this implementation is the high rate at which it must be expanded. A pronounced implementation requires a major reorientation, organization, and change of mindset of industries (manufacturing and chemical), as these demand a large dependence on energy (electricity and heat). Therefore, they demonstrated the considerable potential of DAC using char, but also highlighted numerous challenges that require caution and further targeted analyses.

Zolfaghari et al. [235] reported that although the technology readiness level (TRL) of DAC is at the demonstration stage, identifying commercialization gaps and potential opportunities can aid in the diffusion, adoption, and establishment of this technology. In this research, the authors used databases and data mining (bibliometric analysis) to understand the state-of-the-art, future prospects, and development of DAC from a commercial optical perspective, and identified some more problematic areas. Bibliometric analysis showed that DAC has not yet reached an adequate level of maturity when compared to other existing carbon capture and storage technologies (CCST). They demonstrated that: (i) new systematic designs, improvement in nanocatalysts, increase in capture capacity, (ii) economic and investment improvements in combination with environmental assessment of the optimized DAC technology, (iii) future perspectives, (iv) integration with other alternative energy sources (renewable energy) to meet the energy needs and integration with current carbon emission processes, (v) technology demonstration and readiness assessment, and (vi) analysis of policy and market uncertainties are the primary areas that need to be rigorously explored for the success and implementation of this technology in a highly competitive market.

According to Fasihi et al. [236], despite technological advances, there are still misconceptions about the current and long-term costs of DAC, as well as the demands on energy

consumption, water consumption and location area. The authors highlighted this as a possible compromise of the expected role of DAC in a neutral or negative GEEs system, influencing policy makers. They performed techno-economic analyses of DAC technologies, which were categorized as high-temperature solutions and low-temperature systems from an energy perspective. Capital expenditures, energy demands, and DAC costs were estimated in two scenarios for DAC capacities, and financial learning rates were measured over the period 2020–2050. The costs of the DAC system could be significantly reduced with commercialization in 2020, followed by intensive deployment in 2040 and 2050, making them cost-competitive with point carbon capture and an affordable climate change mitigation solution. They concluded that these new findings positively enhance the role of DAC, presenting successful strategies for further mitigation of climate change.

Based on a critical analysis of the various studies presented in this section, some important points still deserve full attention so that highly operational strategies can be implemented, for example:

(a) The just energy transition between the energy and industrial sectors can be better smoothed;
(b) Socioenvironmental benefits can be supported with more everyday practices in the population's lives;
(c) Socioenvironmental and economic aspects, such as detrimental factors, can be considerably mitigated through the adoption of public policies;
(d) The high capital costs of implementing DACs can be addressed more specifically and quantified;
(e) The problems in developing DACs from a commercial perspective can be addressed through bilateral agreements between countries interested in this technology;
(f) Successful strategies for implementing DACs can be more widely quantified and disseminated.

This section also proposes some concrete strategies to mitigate certain parameters, for example, moisture sensitivity, feedstock variability, and technoeconomic optimization:

Moisture Sensitivity:

(a) Hybrid SST—dehumidification system: develop projects that integrate supersaturated steam treatment (SST) technologies with dehumidification systems to minimize the influence of moisture on process efficiency;
(b) Moisture control: implement real-time humidity control systems to monitor and adjust process operating conditions [231,237].

Feedstock variability:

(a) Residual biomass supply chains: establish policy frameworks to ensure compliance with regulations such as RED II (Renewable Energy Directive II) and promote sustainability in the residual biomass supply chain;
(b) Biomass characterization: perform detailed analyses of biomass to understand better its physicochemical properties, morphostructural characteristics, and thermal behavior, enabling process adjustments to optimize efficiency [238].

Technical-economic optimization:

(a) Coal reactivation energy: conduct technical-economic optimization studies to minimize the energy required for coal reactivation and reduce operating costs.
(b) Life cycle analysis: conduct life cycle analyses to assess the environmental and economic impact of different design and operation options [25].

It is important to note that all of these strategies can be implemented together or separately to mitigate the challenges associated with DAC implementation, ensuring the efficiency and sustainability of the entire process on a smaller or even industrial scale.

Finally, among the different researchers consulted in this review article, a considerable number were unanimous in reporting that the implementation of DAC from PC and GC presented positive and negative aspects, challenges, and limitations. Among these, the following can be listed: physicochemical properties, thermal behavior, non-homogeneity in the structural and morphological characteristics of lignocellulosic biomass, char production processes, and functionalization methods. From a socioeconomic perspective, this study has exposed opportunities that may be useful to address the technical-economic challenges associated with these materials through a combination of experimental techniques and technical-economic evaluations. It is interesting to note that with the knowledge provided here it was possible to present guidelines on the design and implementation of DAC technologies based on scalable and energy-efficient production, facilitating a successful, coherent, and reliable application in industrial settings, which may possibly help global initiatives for CO_2 mitigation.

6. Research Outlook and Future Directions

The application of PCs and GCs for DAC of CO_2 is still in its early stages. Although numerous studies confirm their potential, research remains largely on a laboratory scale and lacks standardization in testing conditions and material design [8,11,86,239–245].

The fundamental advantage of char lies in its low production cost, environmental compatibility, high porosity, and adaptability of properties depending on feedstock and process conditions [240,241]. However, current research is fragmented and primarily lab-scale, with little consensus on optimal material properties or operational conditions under ambient air settings. Thus, future research should prioritize systematic investigations that compare chars in realistic DAC scenarios, especially those involving low CO_2 concentrations (~400 ppm), humidity variations and dynamic capture–regeneration cycles.

A clear future direction is the optimization of activation strategies to enhance the surface area and porosity of chars while maintaining stability and minimizing energy input. Chemical activation, particularly with KOH, has repeatedly shown superior improvements in specific surface area, micropore development, and CO_2 capture capacity [86,242]. However, activation with KOH and other chemicals remains cost- and energy-intensive. Hybrid methods (e.g., KOH followed by CO_2 activation) and emerging microwave-assisted pyrolysis offer promising alternatives, providing greater control over pore structures and allowing the development of graded microporous/mesoporous frameworks. However, the scalability and economic feasibility of these techniques must be further validated through life cycle and techno-economic assessments.

Another critical area is the functionalization of char surfaces with heteroatoms such as nitrogen and sulfur. N-doped and S-doped carbons introduce basic sites and defects, which significantly improve CO_2 adsorption through chemisorption mechanisms [86,239]. In particular, dual doping has demonstrated synergistic effects, improving not only the number of active sites but also the selectivity towards CO_2 under low partial pressure conditions. Future work should explore cost-effective precursors for doping (e.g., sewage sludge, algae, or chitosan [86,239]), while assessing long-term durability and regeneration potential of sorbents. Furthermore, the influence of co-existing gases (e.g., H_2O, O_2, N_2) on doped char performance in DAC systems must be better understood.

Relative humidity presents both a challenge and an opportunity. Although high humidity typically reduces the CO_2 adsorption capacity of some chars, certain porous structures doped with N have demonstrated enhanced performance in humid air [240]. There-

fore, more systematic studies are needed to determine the role of water vapor in modifying sorption equilibria, sorbent degradation, and regeneration pathways under DAC conditions. Incorporating hydrophobic surface treatments or tailoring pore hydrophilicity may offer solutions to moisture-related performance losses.

Feedstock selection and process integration are additional key research vectors. Studies show that digestate solids, sludge, agricultural residues, and waste biomass can be effectively converted to DAC sorbents with reasonable capture capacities and environmental benefits [11,241,242]. Integrating char production with waste valorization or biogas systems could support circular carbon strategies while simultaneously lowering material costs and environmental footprints. However, variability in precursor composition requires a better understanding of how the ash content, inorganic impurities, and volatiles affect the long-term performance of the resulting chars in DAC.

From a mechanistic standpoint, more detailed investigations of adsorption kinetics, pore diffusion mechanisms, and surface interaction energetics (e.g., via in-situ FTIR, XPS, or DFT modeling) are needed to bridge the gap between empirical performance and theoretical understanding. In particular, the working capacity of char-based sorbents (i.e., CO_2 adsorbed/desorbed per cycle) should be emphasized over total capacity in future benchmarking studies, especially under dynamic DAC conditions [239].

Pilot-scale demonstrations, environmental impact assessments, and integration with carbon conversion technologies (e.g., fuel synthesis, mineralization) are essential to translate the promising laboratory-scale findings into industrial DAC applications. As highlighted in [239], few studies have addressed the dynamic behavior of char-based materials during multi-cycle capture and regeneration. In addition, there is a strong need to develop structure–performance–cost models, potentially through machine learning, to guide material design and process optimization.

Future studies should focus on identifying viable commercialization pathways, including the integration of char-DAC systems into existing industrial infrastructure, and evaluating site-specific deployment scenarios. Most existing DAC installations are small-scale and located in Europe, the U.S., and Canada, primarily targeting CO_2 reuse in applications such as carbonated beverages, greenhouses, and synthetic fuel production. Integration with the carbon utilization sectors, such as enhanced oil recovery and urea production, offers practical short-term avenues for deployment [245]. Additionally, combining DAC with bioenergy systems (e.g., BECCS–DAC) presents an opportunity to improve cost-effectiveness and net CO_2 removal. Regulatory support, voluntary carbon markets, and financial incentives such as tax credits will be critical to enabling commercial uptake.

Accurate estimates of capital (CAPEX) and operating (OPEX) costs for large-scale char-based DAC systems are essential. These should account for the activation energy, the replacement of sorbents, and the regeneration demands. Although some companies anticipate future costs below USD 100 per tCO_2, most projections based on available data suggest a more realistic range of USD 100 to 300 per tCO_2 [246]. Performing the lower end of this range will require significant advances in the integration of sorbent materials, process integration, and manufacturing efficiency. The contactor unit—especially the sorbent design—offers major opportunities for cost reduction. Coordinated investment in R&D, infrastructure and techno-economic assessments is necessary to guide viable scale-up pathways [247].

The long-term durability of the sorbent must be repeated adsorption–desorption cycles. In parallel, char-DAC technologies must be evaluated against regulatory frameworks to determine eligibility for carbon offset credits, particularly when using waste-derived feedstocks. The thermodynamic and chemical stability of the sorbent is critical for sustained performance, especially under harsh regeneration conditions that can involve elevated temperatures or reactive environments [25]. Functionalized chars, such as those

doped with nitrogen or amine groups, must retain their active surface sites without degradation or leaching over multiple cycles. Moreover, potential irreversible degradation mechanisms, such as oxidation, thermal decomposition, or reactions with trace atmospheric components such as ozone [98], should be systematically investigated to ensure structural integrity and long-term viability in industrial applications of DAC.

In addition to optimizing CO_2 adsorption capacity, future research should place greater emphasis on the regeneration potential and long-term stability of pyrolysis and gasification chars. For DAC applications, sorbents must withstand multiple adsorption–desorption cycles under ambient or slightly elevated conditions without significant structural degradation or loss of performance. While promising CO_2 uptake values have been reported, very few studies have assessed the durability or recyclability of these materials over time. Investigations of the thermal, mechanical, and chemical stability of modified chars, especially after chemical activation or surface functionalization, are essential to evaluate their viability in continuous DAC operations. Understanding regeneration mechanisms and degradation pathways will be key to designing robust and cost-effective sorbents suitable for real-world deployment.

A summary of key research priorities and future directions is illustrated in Figure 5.

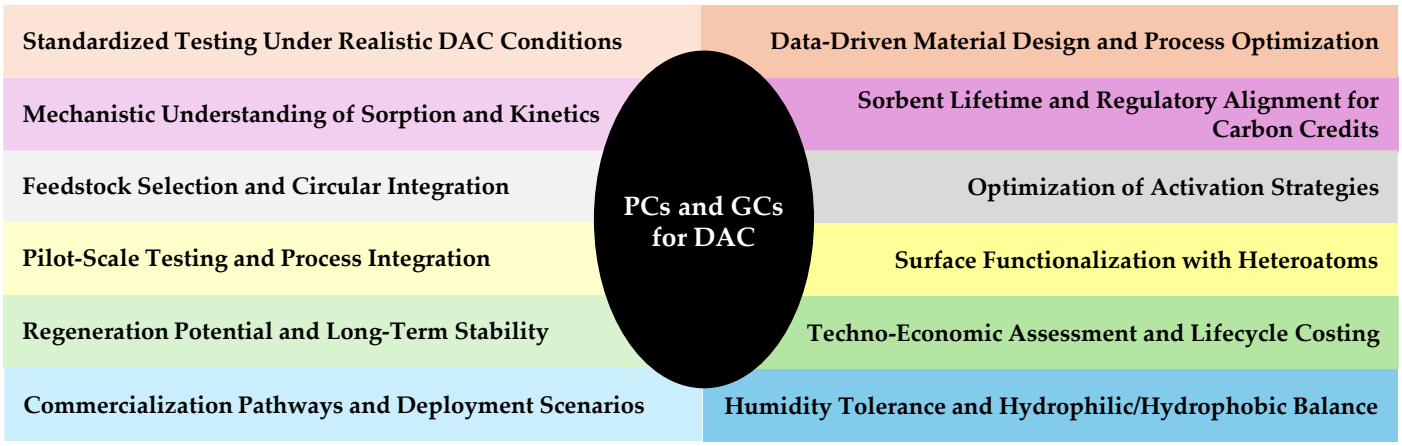

Figure 5. Key research directions for advancing the application of pyrolysis and gasification chars in Direct Air Capture (DAC) of CO_2.

Supplementary Materials: The following supporting information can be downloaded at: https://www.mdpi.com/article/10.3390/en18154120/s1, Figure S1: Comparison of the literature BET surface values.

Author Contributions: Conceptualization, W.J.; software, W.J.; resources, W.J., D.C.d.S. and G.C.; writing—original draft preparation, W.J., B.L., D.C.d.S. and G.C.; writing—review and editing, W.J.; visualization, W.J.; supervision, G.C.; project administration, W.J. and G.C.; funding acquisition, W.J. and G.C. All authors have read and agreed to the published version of the manuscript.

Funding: This research was supported by the program "Excellence Initiative—Research University" for the AGH University of Krakow. The authors also acknowledge the financial support from Brazilian research funding agency: Foundation for Research Support, Scientific, and Technological Development of Maranhão State (FAPEMA), Brazil, grant number 06776/2022.

Data Availability Statement: Not applicable.

Conflicts of Interest: The authors declare no conflicts of interest.

References

1. International Energy Agancy (IEA). Global Energy Review 2025, Paris. Available online: https://www.iea.org/reports/global-energy-review-2025 (accessed on 14 April 2025).
2. Lan, X.; Tans, P.; Thoning, K.W. Trends in Globally-Averaged CO_2 Determined from NOAA Global Monitoring Laboratory Measurements. Available online: https://doi.org/10.15138/9N0H-ZH07 (accessed on 5 May 2025).
3. Wu, C.; Huang, Q.; Xu, Z.; Sipra, A.T.; Gao, N.; Vandenberghe, L.P.d.S.; Vieira, S.; Soccol, C.R.; Zhao, R.; Deng, S.; et al. A Comprehensive Review of Carbon Capture Science and Technologies. *Carbon Capture Sci. Technol.* **2024**, *11*, 100178. https://doi.org/10.1016/j.ccst.2023.100178.
4. Ghaffari, S.; Gutierrez, M.F.; Seidel-Morgenstern, A.; Lorenz, H.; Schulze, P. Sodium Hydroxide-Based CO_2 Direct Air Capture for Soda Ash Production-Fundamentals for Process Engineering. *Ind. Eng. Chem. Res.* **2023**, *62*, 7566–7579. https://doi.org/10.1021/acs.iecr.3c00357.
5. Zolfaghari, Z.; Aslani, A.; Zahedi, R.; Kazzazi, S. Simulation of Carbon Dioxide Direct Air Capture Plant Using Potassium Hydroxide Aqueous Solution: Energy Optimization and CO_2 Purity Enhancement. *Energy Convers. Manag. X* **2024**, *21*, 100489. https://doi.org/10.1016/j.ecmx.2023.100489.
6. An, K.; Li, K.; Yang, C.M.; Brechtl, J.; Stamberga, D.; Zhang, M.; Nawaz, K. Direct Air Capture with Amino Acid Solvent: Operational Optimization Using a Crossflow Air-Liquid Contactor. *AIChE J.* **2024**, *70*, e18429. https://doi.org/10.1002/aic.18429.
7. Hua, J.; Shen, X.; Jiao, X.; Lin, H.; Li, G.; Sun, X.; Yan, F.; Wu, H.; Zhang, Z. Direct Air Capture of CO_2 by Amine-Impregnated Resin: The Effect of Resin Pore Structure and Humid Conditions. *Carbon Capture Sci. Technol.* **2024**, *12*, 100237. https://doi.org/10.1016/j.ccst.2024.100237.
8. Priyadarshini, P.; Rim, G.; Rosu, C.; Song, M.G.; Jones, C.W. Direct Air Capture of CO_2 Using Amine/Alumina Sorbents at Cold Temperature. *ACS Environ. Au* **2023**, *3*, 295–307. https://doi.org/10.1021/acsenvironau.3c00010.
9. Schellevis, H.M.; Brilman, D.W.F. Experimental Study of CO_2 Capture from Air via Steam-Assisted Temperature-Vacuum Swing Adsorption with a Compact Kg-Scale Pilot Unit. *React. Chem. Eng.* **2024**, *9*, 910–924. https://doi.org/10.1039/d3re00460k.
10. Shi, W.K.; Zhang, X.J.; Liu, X.; Wei, S.; Shi, X.; Wu, C.; Jiang, L. Temperature-Vacuum Swing Adsorption for Direct Air Capture by Using Low-Grade Heat. *J. Clean. Prod.* **2023**, *414*, 137731. https://doi.org/10.1016/j.jclepro.2023.137731.
11. Liu, J.; Wang, Z.; Liang, C.; Fang, K.; Li, S.; Guo, X.; Wang, T.; Fang, M. Direct Air Capture of CO_2 Using Biochar Prepared from Sewage Sludge: Adsorption Capacity and Kinetics. *Sci. Total Environ.* **2024**, *948*, 174887. https://doi.org/10.1016/j.scitotenv.2024.174887.
12. Li, L.; Xiao, Z.; Xu, C.; Zhou, Y.; Li, Z. The Utility of MOF-Based Materials in Direct Air Capture (DAC) Application to Ppm-Level CO_2. *Environ. Res.* **2024**, *262*, 119985. https://doi.org/10.1016/j.envres.2024.119985.
13. Xiang, X.; Guo, T.; Yin, Y.; Gao, Z.; Wang, Y.; Wang, R.; An, M.; Guo, Q.; Hu, X. High Adsorption Capacity Fe@13X Zeolite for Direct Air CO_2 Capture. *Ind. Eng. Chem. Res.* **2023**, *62*, 5420–5429. https://doi.org/10.1021/acs.iecr.2c04458.
14. Seo, H.; Hatton, T.A. Electrochemical Direct Air Capture of CO_2 Using Neutral Red as Reversible Redox-Active Material. *Nat. Commun.* **2023**, *14*, 313. https://doi.org/10.1038/s41467-023-35866-w.
15. Chae, J.E.; Choi, J.; Lee, D.; Lee, S.; Kim, S. Development of Anion Exchange Membrane-Based Electrochemical CO_2 Separation Cells for Direct Air Capture. *J. Ind. Eng. Chem.* **2024**, *145*, 543–550. https://doi.org/10.1016/j.jiec.2024.10.049.
16. Ji, Y.; Liu, W.; Yong, J.Y.; Zhang, X.J.; Jiang, L. Techno-Economic Analysis on Temperature Vacuum Swing Adsorption System Integrated with Pre-Dehumidification for Direct Air Capture. *Carbon Capture Sci. Technol.* **2024**, *12*, 100199. https://doi.org/10.1016/j.ccst.2024.100199.
17. Grossmann, Q.; Stampi-Bombelli, V.; Yakimov, A.; Docherty, S.; Copéret, C.; Mazzotti, M. Developing Versatile Contactors for Direct Air Capture of CO_2 through Amine Grafting onto Alumina Pellets and Alumina Wash-Coated Monoliths. *Ind. Eng. Chem. Res.* **2023**, *62*, 13594–13611. https://doi.org/10.1021/acs.iecr.3c01265.
18. Sabatino, F.; Mehta, M.; Grimm, A.; Gazzani, M.; Gallucci, F.; Kramer, G.J.; Van Sint Annaland, M. Evaluation of a Direct Air Capture Process Combining Wet Scrubbing and Bipolar Membrane Electrodialysis. *Ind. Eng. Chem. Res.* **2020**, *59*, 7007–7020. https://doi.org/10.1021/acs.iecr.9b05641.
19. Barahimi, V.; Ho, M.; Croiset, E. From Lab to Fab: Development and Deployment of Direct Air Capture of CO_2. *Energies* **2023**, *16*, 6385. https://doi.org/10.3390/en16176385.
20. Kiani, A.; Conway, W.; Abdellah, M.H.; Puxty, G.; Minor, A.J.; Kluivers, G.; Bennett, R.; Feron, P. A Study on Degradation and CO_2 Capture Performance of Aqueous Amino Acid Salts for Direct Air Capture Applications. *Greenh. Gases Sci. Technol.* **2024**, *870*, 859–870. https://doi.org/10.1002/ghg.2302.

21. Ali, K.; Mohamed, H.A.; Ali, P.; Paul, F. Amine Based Liquid Capture Technology for Direct Air Capture of CO_2—An Overview on Technology Development. *Aust. Energy Prod. J.* **2025**, *65*, EP24224. https://doi.org/10.1071/EP24224.
22. Wang, E.; Luo, L.; Wang, J.; Dai, J.; Li, S.; Chen, L.; Li, J. A Dataset for Investigations of Amine-Impregnated Solid Adsorbent for Direct Air Capture. *Sci. Data* **2025**, *12*, 724. https://doi.org/10.1038/s41597-025-05037-1.
23. Jin, Y.; Lin, H.; Liu, Y.; An, H.; Lee, J.S. Optimizing Amine-Based Adsorbents for Direct Air Capture: A Comprehensive Review of Performance under Diverse Climatic Conditions. *Renew. Sustain. Energy Rev.* **2025**, *217*, 115782. https://doi.org/10.1016/j.rser.2025.115782.
24. Sanz-Pérez, E.S.; Murdock, C.R.; Didas, S.A.; Jones, C.W. Direct Capture of CO_2 from Ambient Air. *Chem. Rev.* **2016**, *116*, 11840–11876. https://doi.org/10.1021/acs.chemrev.6b00173.
25. Zentou, H.; Hoque, B.; Abdalla, M.A.; Saber, A.F.; Abdelaziz, O.Y.; Aliyu, M.; Alkhedhair, A.M.; Alabduly, A.J.; Abdelnaby, M.M. Recent Advances and Challenges in Solid Sorbents for CO_2 Capture. *Carbon Capture Sci. Technol.* **2025**, *15*, 100386. https://doi.org/10.1016/j.ccst.2025.100386.
26. Stampi-Bombelli, V.; Storione, A.; Grossmann, Q.; Mazzotti, M. On Comparing Packed Beds and Monoliths for CO_2 Capture from Air Through Experiments, Theory, and Modeling. *Ind. Eng. Chem. Res.* **2024**, *63*, 11637–11653. https://doi.org/10.1021/acs.iecr.4c01392.
27. Ooi, B.K.H.; Marek, E.J. Kinetics of CO_2 Capture with Calcium Oxide during Direct Air Capture in a Fluidized Bed. *Energy Fuels* **2024**, *38*, 22290–22297. https://doi.org/10.1021/acs.energyfuels.4c03770.
28. Europian Commission. *Directive (EU) 2018/2001 of the European Parliament and of the Council of 11 December 2018 on the Promotion of the Use of Energy from Renewable*; Europian Commission: Brussels, Belgium, 2018.
29. Laeim, H.; Molahalli, V.; Prajongthat, P.; Pattanaporkratana, A.; Pathak, G.; Phettong, B.; Hongkarnjanakul, N.; Chattham, N. Porosity Tunable Metal-Organic Framework (MOF)-Based Composites for Energy Storage Applications: Recent Progress. *Polymers* **2025**, *17*, 130. https://doi.org/10.3390/polym17020130.
30. Pérez-Botella, E.; Valencia, S.; Rey, F. Zeolites in Adsorption Processes: State of the Art and Future Prospects. *Chem. Rev.* **2022**, *122*, 17647–17695. https://doi.org/10.1021/acs.chemrev.2c00140.
31. Ozden, A. CO_2 Capture via Electrochemical PH-Mediated Systems. *ACS Energy Lett.* **2025**, *10*, 1550–1576. https://doi.org/10.1021/acsenergylett.5c00200.
32. Sevilla, M.; Fuertes, A.B. Sustainable Porous Carbons with a Superior Performance for CO_2 Capture. *Energy Environ. Sci.* **2011**, *4*, 1765–1771. https://doi.org/10.1039/c0ee00784f.
33. Li, K.; Zhang, D.; Niu, X.; Guo, H.; Yu, Y.; Tang, Z.; Lin, Z.; Fu, M. Insights into CO_2 Adsorption on KOH-Activated Biochars Derived from the Mixed Sewage Sludge and Pine Sawdust. *Sci. Total Environ.* **2022**, *826*, 154133. https://doi.org/10.1016/j.scitotenv.2022.154133.
34. Yang, X.; Wang, H.; Strong, P.J.; Xu, S.; Liu, S.; Lu, K.; Sheng, K.; Guo, J.; Che, L.; He, L.; et al. Thermal Properties of Biochars Derived from Waste Biomass Generated by Agricultural and Forestry Sectors. *Energies* **2017**, *10*, 469. https://doi.org/10.3390/en10040469.
35. Miskolczi, N.; Gao, N.; Quan, C.; Laszlo, A.T. CO_2 Reduction by Chars Obtained by Pyrolysis of Real Wastes: Low Temperature Adsorption and High Temperature CO_2 Capture. *Carbon Capture Sci. Technol.* **2025**, *14*, 100332. https://doi.org/10.1016/j.ccst.2024.100332.
36. Brebu, M.; Ioniță, D.; Stoleru, E. Thermal Behavior and Conversion of Agriculture Biomass Residues by Torrefaction and Pyrolysis. *Sci. Rep.* **2025**, *15*, 11505. https://doi.org/10.1038/s41598-025-88001-8.
37. Faizan, M.; Song, H. Critical Review on Catalytic Biomass Gasification: State-of-Art Progress, Technical Challenges, and Perspectives in Future Development. *J. Clean. Prod.* **2024**, *408*, 137224. https://doi.org/10.1016/j.jclepro.2023.137224.
38. Vuppaladadiyam, A.K.; Varsha Vuppaladadiyam, S.S.; Sikarwar, V.S.; Ahmad, E.; Pant, K.K.; S, M.; Pandey, A.; Bhattacharya, S.; Sarmah, A.; Leu, S.Y. A Critical Review on Biomass Pyrolysis: Reaction Mechanisms, Process Modeling and Potential Challenges. *J. Energy Inst.* **2023**, *108*, 101236. https://doi.org/10.1016/j.joei.2023.101236.
39. Lataf, A.; Jozefczak, M.; Vandecasteele, B.; Viaene, J.; Schreurs, S.; Carleer, R.; Yperman, J.; Marchal, W.; Cuypers, A.; Vandamme, D. The Effect of Pyrolysis Temperature and Feedstock on Biochar Agronomic Properties. *J. Anal. Appl. Pyrolysis* **2022**, *168*, 105728. https://doi.org/10.1016/j.jaap.2022.105728.
40. Anand, A.; Gautam, S.; Ram, L.C. Feedstock and Pyrolysis Conditions Affect Suitability of Biochar for Various Sustainable Energy and Environmental Applications. *J. Anal. Appl. Pyrolysis* **2023**, *170*, 105881. https://doi.org/10.1016/j.jaap.2023.105881.
41. Khater, E.S.; Bahnasawy, A.; Hamouda, R.; Sabahy, A.; Abbas, W.; Morsy, O.M. Biochar Production under Different Pyrolysis Temperatures with Different Types of Agricultural Wastes. *Sci. Rep.* **2024**, *14*, 2625. https://doi.org/10.1038/s41598-024-52336-5.

42. Parthasarathy, P.; Mackey, H.R.; Mariyam, S.; Zuhara, S.; Al-Ansari, T.; McKay, G. Char Products From Bamboo Waste Pyrolysis and Acid Activation. *Front. Mater.* **2021**, *7*, 624791. https://doi.org/10.3389/fmats.2020.624791.
43. Huang, G.G.; Liu, Y.F.; Wu, X.X.; Cai, J.J. Activated Carbons Prepared by the KOH Activation of a Hydrochar from Garlic Peel and Their CO_2 Adsorption Performance. *New Carbon Mater.* **2019**, *34*, 247–257. https://doi.org/10.1016/S1872-5805(19)60014-4.
44. Shahkarami, S.; Azargohar, R.; Dalai, A.K.; Soltan, J. Breakthrough CO_2 Adsorption in Bio-Based Activated Carbons. *J. Environ. Sci.* **2015**, *34*, 68–76. https://doi.org/10.1016/j.jes.2015.03.008.
45. Jerzak, W.; Mlonka-Mędrala, A.; Gao, N.; Magdziarz, A. Potential of Products from High-Temperature Pyrolysis of Biomass and Refuse-Derived Fuel Pellets. *Biomass Bioenergy* **2024**, *183*, 107159. https://doi.org/10.1016/j.biombioe.2024.107159.
46. Wang, K.; Xu, S. Preparation of High Specific Surface Area Activated Carbon from Petroleum Coke by KOH Activation in a Rotary Kiln. *Processes* **2024**, *12*, 241. https://doi.org/10.3390/pr12020241.
47. Fu, Y.; Shen, Y.; Zhang, Z.; Ge, X.; Chen, M. Activated Bio-Chars Derived from Rice Husk via One- and Two-Step KOH-Catalyzed Pyrolysis for Phenol Adsorption. *Sci. Total Environ.* **2019**, *646*, 1567–1577. https://doi.org/10.1016/j.scitotenv.2018.07.423.
48. Zhang, C.; Ji, Y.; Li, C.; Zhang, Y.; Sun, S.; Xu, Y.; Jiang, L.; Wu, C. The Application of Biochar for CO_2 Capture: Influence of Biochar Preparation and CO_2 Capture Reactors. *Ind. Eng. Chem. Res.* **2023**, *62*, 17168–17181. https://doi.org/10.1021/acs.iecr.3c00445.
49. Aissaoui, M.H.; Hertzog, J.; Sambusiti, C.; Gauthier-Maradei, P.; Pons, M.N.; Carré, V.; Brech, Y.L.; Dufour, A. Thermochemical Conversion of Solid Digestates: Effects of Temperature and Fluidizing Gas on Products Composition. *J. Anal. Appl. Pyrolysis* **2025**, *186*, 106928. https://doi.org/10.1016/j.jaap.2024.106928.
50. Yue, Y.; Jin, X.; Deng, L. Experimental Study on Properties of Syngas, Tar, and Biochar Derived from Different Gasification Methods. *Appl. Sci.* **2023**, *13*, 11490. https://doi.org/10.3390/app132011490.
51. Hansen, V.; Müller-Stöver, D.; Ahrenfeldt, J.; Holm, J.K.; Henriksen, U.B.; Hauggaard-Nielsen, H. Gasification Biochar as a Valuable By-Product for Carbon Sequestration and Soil Amendment. *Biomass Bioenergy* **2015**, *72*, 300–308. https://doi.org/10.1016/j.biombioe.2014.10.013.
52. Sieradzka, M.; Mlonka, -M.A.; Kalemba-Rec, I.; Reinmöller, M.; Kuster, F.; Kalawa, W.; Magdziarz, A. Evaluation of Physical and Chemical Properties of Residue from Gasification of Biomass Wastes. *Energies* **2022**, *15*, 3539. https://doi.org/10.3390/en15103539.
53. Klinghoffer, N.B.; Castaldi, M.J.; Nzihou, A. Catalyst Properties and Catalytic Performance of Char from Biomass Gasification. *Ind. Eng. Chem. Res.* **2012**, *51*, 13113–13122. https://doi.org/10.1021/ie3014082.
54. Benedetti, V.; Cordioli, E.; Patuzzi, F.; Baratieri, M. CO_2 Adsorption Study on Pure and Chemically Activated Chars Derived from Commercial Biomass Gasifiers. *J. CO_2 Util.* **2019**, *33*, 46–54.
55. Dissanayake, P.D.; Choi, S.W.; Igalavithana, A.D.; Yang, X.; Tsang, D.C.W.; Wang, C.H.; Kua, H.W.; Lee, K.B.; Ok, Y.S. Sustainable Gasification Biochar as a High Efficiency Adsorbent for CO_2 Capture: A Facile Method to Designer Biochar Fabrication. *Renew. Sustain. Energy Rev.* **2020**, *124*, 109785. https://doi.org/10.1016/j.rser.2020.109785.
56. Zhu, D.; Wang, Q.; Xie, G.; Ye, Z.; Zhu, Z.; Ye, C. Effect of Air Equivalence Ratio on the Characteristics of Biomass Partial Gasification for Syngas and Biochar Co-Production in the Fluidized Bed. *Renew. Energy* **2024**, *222*, 119881. https://doi.org/10.1016/j.renene.2023.119881.
57. Edeh, I.G.; Masek, O.; Fusseis, F. 4D Structural Changes and Pore Network Model of Biomass during Pyrolysis. *Sci. Rep.* **2023**, *13*, 22863. https://doi.org/10.1038/s41598-023-49919-z.
58. Muzyka, R.; Misztal, E.; Hrabak, J.; Banks, S.W.; Sajdak, M. Various Biomass Pyrolysis Conditions Influence the Porosity and Pore Size Distribution of Biochar. *Energy* **2023**, *263*, 126128. https://doi.org/10.1016/j.energy.2022.126128.
59. Ding, S.; Kantarelis, E.; Engvall, K. Effects of Porous Structure Development and Ash on the Steam Gasification Reactivity of Biochar Residues from a Commercial Gasifier at Different Temperatures. *Energies* **2020**, *13*, 5004. https://doi.org/10.3390/en13195004.
60. Wu, R.; Beutler, J.; Price, C.; Baxter, L.L. Biomass Char Particle Surface Area and Porosity Dynamics during Gasification. *Fuel* **2020**, *264*, 116833. https://doi.org/10.1016/j.fuel.2019.116833.
61. Surup, G.R.; Trubetskaya, A.; Tangstad, M. Charcoal as an Alternative Reductant in Ferroalloy Production: A Review. *Processes* **2020**, *8*, 1432. https://doi.org/10.3390/pr8111432.
62. Abdelaal, A.; Benedetti, V.; Villot, A.; Patuzzi, F.; Gerente, C.; Baratieri, M. Innovative Pathways for the Valorization of Biomass Gasification Char: A Systematic Review. *Energies* **2023**, *16*, 4175. https://doi.org/10.3390/en16104175.

63. Chen, J.; Ding, L.; Wang, P.; Zhang, W.; Li, J.; Mohamed, B.A.; Chen, J.; Leng, S.; Liu, T.; Leng, L.; et al. The Estimation of the Higher Heating Value of Biochar by Data-Driven Modeling. *J. Renew. Mater.* **2022**, *10*, 1555–1574. https://doi.org/10.32604/jrm.2022.018625.
64. Enders, A.; Hanley, K.; Whitman, T.; Joseph, S.; Lehmann, J. Characterization of Biochars to Evaluate Recalcitrance and Agronomic Performance. *Bioresour. Technol.* **2012**, *114*, 644–653. https://doi.org/10.1016/j.biortech.2012.03.022.
65. Ahmad, A.A.; Ahmad, M.A.; Md Ali, U.F.; Ken, K. Gasification Char Residues Management: Assessing the Characteristics for Adsorption Application. *Arab. J. Chem.* **2023**, *16*, 104993. https://doi.org/10.1016/j.arabjc.2023.104993.
66. Hernández, J.J.; Lapuerta, M.; Monedero, E. Characterisation of Residual Char from Biomass Gasification: Effect of the Gasifier Operating Conditions. *J. Clean. Prod.* **2016**, *138*, 83–93. https://doi.org/10.1016/j.jclepro.2016.05.120.
67. Usman, A.R.A.; Abduljabbar, A.; Vithanage, M.; Ok, Y.S.; Ahmad, M.M.; Ahmad, M.M.; Elfaki, J.; Abdulazeem, S.S.; Al-Wabel, M.I. Biochar Production from Date Palm Waste: Charring Temperature Induced Changes in Composition and Surface Chemistry. *J. Anal. Appl. Pyrolysis* **2015**, *115*, 392–400. https://doi.org/10.1016/j.jaap.2015.08.016.
68. Wanignon Ferdinand, F.; Van De Steene, L.; Kamenan Blaise, K.; Siaka, T. Prediction of Pyrolysis Oils Higher Heating Value with Gas Chromatography-Mass Spectrometry. *Fuel* **2012**, *96*, 141–145. https://doi.org/10.1016/j.fuel.2012.01.007.
69. Suresh Babu, K.K.B.; Nataraj, M.; Tayappa, M.; Vyas, Y.; Mishra, R.K.; Acharya, B. Production of Biochar from Waste Biomass Using Slow Pyrolysis: Studies of the Effect of Pyrolysis Temperature and Holding Time on Biochar Yield and Properties. *Mater. Sci. Energy Technol.* **2024**, *7*, 318–334. https://doi.org/10.1016/j.mset.2024.05.002.
70. Adhikari, S.; Moon, E.; Paz-Ferreiro, J.; Timms, W. Comparative Analysis of Biochar Carbon Stability Methods and Implications for Carbon Credits. *Sci. Total Environ.* **2024**, *914*, 169607. https://doi.org/10.1016/j.scitotenv.2023.169607.
71. Qian, K.; Kumar, A.; Patil, K.; Bellmer, D.; Wang, D.; Yuan, W.; Huhnke, R.L. Effects of Biomass Feedstocks and Gasification Conditions on the Physiochemical Properties of Char. *Energies* **2013**, *6*, 3972–3986. https://doi.org/10.3390/en6083972.
72. Petersen, H.I.; Sanei, H. The H/C Molar Ratio and Its Potential Pitfalls for Determining Biochar's Permanence. *GCB Bioenergy* **2025**, *17*, e70049. https://doi.org/10.1111/gcbb.70049.
73. Chen, J.; Zhou, J.; Zheng, W.; Leng, S.; Ai, Z.; Zhang, W.; Yang, Z.; Yang, J.; Xu, Z.; Cao, J.; et al. A Complete Review on the Oxygen-Containing Functional Groups of Biochar: Formation Mechanisms, Detection Methods, Engineering, and Applications. *Sci. Total Environ.* **2024**, *946*, 174081. https://doi.org/10.1016/j.scitotenv.2024.174081.
74. Sharma, T.; Hakeem, I.G.; Gupta, A.B.; Joshi, J.; Shah, K.; Vuppaladadiyam, A.K.; Sharma, A. Parametric Influence of Process Conditions on Thermochemical Techniques for Biochar Production: A State-of-the-Art Review. *J. Energy Inst.* **2024**, *113*, 101559. https://doi.org/10.1016/j.joei.2024.101559.
75. Leng, L.; Xu, S.; Liu, R.; Yu, T.; Zhuo, X.; Leng, S.; Xiong, Q.; Huang, H. Nitrogen Containing Functional Groups of Biochar: An Overview. *Bioresour. Technol.* **2020**, *298*, 122286. https://doi.org/10.1016/j.biortech.2019.122286.
76. Zhou, J.; Masutani, S.M.; Ishimura, D.M.; Turn, S.Q.; Kinoshita, C.M. Release of Fuel-Bound Nitrogen during Biomass Gasification. *Ind. Eng. Chem. Res.* **2000**, *39*, 626–634. https://doi.org/10.1021/ie980318o.
77. Soo, X.Y.D.; Lee, J.J.C.; Wu, W.Y.; Tao, L.; Wang, C.; Zhu, Q.; Bu, J. Advancements in CO_2 Capture by Absorption and Adsorption: A Comprehensive Review. *J. CO_2 Util.* **2024**, *81*, 102727. https://doi.org/10.1016/j.jcou.2024.102727.
78. Petrovic, B.; Gorbounov, M.; Masoudi Soltani, S. Impact of Surface Functional Groups and Their Introduction Methods on the Mechanisms of CO_2 Adsorption on Porous Carbonaceous Adsorbents. *Carbon Capture Sci. Technol.* **2022**, *3*, 100045. https://doi.org/10.1016/j.ccst.2022.100045.
79. Gao, X.; Yang, S.; Hu, L.; Cai, S.; Wu, L.; Kawi, S. Carbonaceous Materials as Adsorbents for CO_2 Capture: Synthesis and Modification. *Carbon Capture Sci. Technol.* **2022**, *3*, 100039. https://doi.org/10.1016/j.ccst.2022.100039.
80. Plaza, M.G.; González, A.S.; Pevida, C.; Pis, J.J.; Rubiera, F. Valorisation of Spent Coffee Grounds as CO_2 Adsorbents for Postcombustion Capture Applications. *Appl. Energy* **2012**, *99*, 272–279. https://doi.org/10.1016/j.apenergy.2012.05.028.
81. Serafin, J.; Narkiewicz, U.; Morawski, A.W.; Wróbel, R.J.; Michalkiewicz, B. Highly Microporous Activated Carbons from Biomass for CO_2 Capture and Effective Micropores at Different Conditions. *J. CO_2 Util.* **2017**, *18*, 73–79. https://doi.org/10.1016/j.jcou.2017.01.006.
82. Li, M.; Xiao, R. Preparation of a Dual Pore Structure Activated Carbon from Rice Husk Char as an Adsorbent for CO_2 Capture. *Fuel Process. Technol.* **2019**, *186*, 35–39. https://doi.org/10.1016/j.fuproc.2018.12.015.
83. Wei, H.; Deng, S.; Hu, B.; Chen, Z.; Wang, B.; Huang, J.; Yu, G. Granular Bamboo-Derived Activated Carbon for High CO_2 Adsorption: The Dominant Role of Narrow Micropores. *ChemSusChem* **2012**, *5*, 2354–2360. https://doi.org/10.1002/cssc.201200570.

84. Hao, W.; Björkman, E.; Lilliestråle, M.; Hedin, N. Activated Carbons Prepared from Hydrothermally Carbonized Waste Biomass Used as Adsorbents for CO_2. *Appl. Energy* **2013**, *112*, 526–532. https://doi.org/10.1016/j.apenergy.2013.02.028.
85. Yang, H.; Gong, M.; Chen, Y. Preparation of Activated Carbons and Their Adsorption Properties for Greenhouse Gases: CH_4 and CO_2. *J. Nat. Gas Chem.* **2011**, *20*, 460–464. https://doi.org/10.1016/S1003-9953(10)60232-0.
86. Chen, J.; Lin, J.; Luo, J.; Tian, Z.; Zhang, J.; Sun, S.; Shen, Y.; Ma, R. Enhanced CO_2 Capture Performance of N, S Co-Doped Biochar Prepared by Microwave Pyrolysis: Synergistic Modulation of Microporous Structure and Functional Groups. *Fuel* **2025**, *379*, 132987. https://doi.org/10.1016/j.fuel.2024.132987.
87. Shao, S.; Wang, Y.; Ma, L.; Huang, Z.; Li, X. Sustainable Preparation of Hierarchical Porous Carbon from Discarded Shells of Crustaceans for Efficient CO_2 Capture. *Fuel* **2024**, *355*, 129287. https://doi.org/10.1016/j.fuel.2023.129287.
88. Wei, H.; Chen, J.; Fu, N.; Chen, H.; Lin, H.; Han, S. Biomass-Derived Nitrogen-Doped Porous Carbon with Superior Capacitive Performance and High CO_2 Capture Capacity. *Electrochim. Acta* **2018**, *266*, 161–169. https://doi.org/10.1016/j.electacta.2017.12.192.
89. Chen, J.; Yang, J.; Hu, G.; Hu, X.; Li, Z.; Shen, S.; Radosz, M.; Fan, M. Enhanced CO_2 Capture Capacity of Nitrogen-Doped Biomass-Derived Porous Carbons. *ACS Sustain. Chem. Eng.* **2016**, *4*, 1439–1445. https://doi.org/10.1021/acssuschemeng.5b01425.
90. Li, D.; Tian, Y.; Li, L.; Li, J.; Zhang, H. Production of Highly Microporous Carbons with Large CO_2 Uptakes at Atmospheric Pressure by KOH Activation of Peanut Shell Char. *J. Porous Mater.* **2015**, *22*, 1581–1588. https://doi.org/10.1007/s10934-015-0041-7.
91. Han, J.; Zhang, L.; Zhao, B.; Qin, L.; Wang, Y.; Xing, F. The N-Doped Activated Carbon Derived from Sugarcane Bagasse for CO_2 Adsorption. *Ind. Crops Prod.* **2019**, *128*, 290–297. https://doi.org/10.1016/j.indcrop.2018.11.028.
92. Xu, J.; Shi, J.; Cui, H.; Yan, N.; Liu, Y. Preparation of Nitrogen Doped Carbon from Tree Leaves as Efficient CO_2 Adsorbent. *Chem. Phys. Lett.* **2018**, *711*, 107–112. https://doi.org/10.1016/j.cplett.2018.09.038.
93. González, A.S.; Plaza, M.G.; Rubiera, F.; Pevida, C. Sustainable Biomass-Based Carbon Adsorbents for Post-Combustion CO_2 Capture. *Chem. Eng. J.* **2013**, *230*, 456–465. https://doi.org/10.1016/j.cej.2013.06.118.
94. Nguyen, H.N.; Khuong, D.A.; Tsubota, T. Experimental Investigation of CO_2 Adsorption Using Adsorbents Derived from Residual Char of Agricultural Waste Gasification. *Therm. Sci. Eng. Prog.* **2024**, *49*, 102446. https://doi.org/10.1016/j.tsep.2024.102446.
95. Rashidi, N.A.; Yusup, S. Production of Palm Kernel Shell-Based Activated Carbon by Direct Physical Activation for Carbon Dioxide Adsorption. *Environ. Sci. Pollut. Res.* **2019**, *26*, 33732–33746. https://doi.org/10.1007/s11356-018-1903-8.
96. Khosrowshahi, M.S.; Mashhadimoslem, H.; Shayesteh, H.; Singh, G.; Khakpour, E.; Guan, X.; Rahimi, M.; Maleki, F.; Kumar, P.; Vinu, A. Natural Products Derived Porous Carbons for CO_2 Capture. *Adv. Sci.* **2023**, *10*, 2304289. https://doi.org/10.1002/advs.202304289.
97. Wiegner, J.F.; Grimm, A.; Weimann, L.; Gazzani, M. Optimal Design and Operation of Solid Sorbent Direct Air Capture Processes at Varying Ambient Conditions. *Ind. Eng. Chem. Res.* **2022**, *61*, 12649–12667. https://doi.org/10.1021/acs.iecr.2c00681.
98. Jamdade, S.; Cai, X.; Sholl, D.S. Assessment of Long-Term Degradation of Adsorbents for Direct Air Capture by Ozonolysis. *J. Phys. Chem. C* **2025**, *129*, 899–909. https://doi.org/10.1021/acs.jpcc.4c07054.
99. Kumar, A.; Singh, E.; Mishra, R.; Lo, S.L.; Kumar, S. A Green Approach towards Sorption of CO_2 on Waste Derived Biochar. *Environ. Res.* **2022**, *214*, 113954. https://doi.org/10.1016/j.envres.2022.113954.
100. Grams, J. Surface Analysis of Solid Products of Thermal Treatment of Lignocellulosic Biomass. *J. Anal. Appl. Pyrolysis* **2022**, *161*, 105429. https://doi.org/10.1016/j.jaap.2021.105429.
101. He, D.; Luo, Y.; Zhu, B. Feedstock and Pyrolysis Temperature Influence Biochar Properties and Its Interactions with Soil Substances: Insights from a DFT Calculation. *Sci. Total Environ.* **2024**, *922*, 171259. https://doi.org/10.1016/j.scitotenv.2024.171259.
102. Li, X.; Huang, Y.; Liang, X.; Huang, L.; Wei, L.; Zheng, X.; Albert, H.A.; Huang, Q.; Liu, Z.; Li, Z. Characterization of Biochars from Woody Agricultural Wastes and Sorption Behavior Comparison of Cadmium and Atrazine. *Biochar* **2022**, *4*, 27. https://doi.org/10.1007/s42773-022-00132-7.
103. Zhang, C.; Wu, L.; Kang, R.; Bin, F.; Dou, B. Precise In-Situ Infrared Spectra and Kinetic Analysis of Gasification under the H_2O or CO_2 Atmospheres. *Int. J. Hydrog. Energy* **2024**, *52*, 46–57. https://doi.org/10.1016/j.ijhydene.2023.01.241.
104. Brewer, C.E.; Unger, R.; Schmidt-Rohr, K.; Brown, R.C. Criteria to Select Biochars for Field Studies Based on Biochar Chemical Properties. *Bioenergy Res.* **2011**, *4*, 312–323. https://doi.org/10.1007/s12155-011-9133-7.
105. Li, B.; Liu, D.; Lin, D.; Xie, X.; Wang, S.; Xu, H.; Wang, J.; Huang, Y.; Zhang, S.; Hu, X. Changes in Biochar Functional Groups and Its Reactivity after Volatile-Char Interactions during Biomass Pyrolysis. *Energy Fuels* **2020**, *34*, 14291–14299. https://doi.org/10.1021/acs.energyfuels.0c03243.

106. Li, B.; Ding, S.; Fan, H.; Ren, Y. Experimental Investigation into the Effect of Pyrolysis on Chemical Forms of Heavy Metals in Sewage Sludge Biochar (SSB), with Brief Ecological Risk Assessment. *Materials* **2021**, *14*, 447. https://doi.org/10.3390/ma14020447.
107. Lahijani, P.; Zainal, Z.A.; Mohamed, A.R.; Mohammadi, M. CO2 Gasification Reactivity of Biomass Char: Catalytic Influence of Alkali, Alkaline Earth and Transition Metal Salts. *Bioresour. Technol.* **2013**, *144*, 288–295. https://doi.org/10.1016/j.biortech.2013.06.059.
108. Echeverria-Paredes, P.; Mood, S.H. *Biomass Thermo-Chemical Products*; Garcia-Perez, M., Chejne-Janna, F., Eds.; Elsevier Inc.: Amsterdam, The Netherlands, 2025; ISBN 9780323955515.
109. Jha, S.; Pattnaik, F.; Zapata, O.; Acharya, B.; Dalai, A.K. KOH-Assisted Chemical Activation of Camelina Meal (Wild Flax) to Treat PFOA-Contaminated Wastewater. *Sustainability* **2025**, *17*, 2170. https://doi.org/10.3390/su17052170.
110. Romero, C.M.; Redman, A.A.P.H.; Terry, S.A.; Hazendonk, P.; Hao, X.; McAllister, T.A.; Okine, E. Molecular Speciation and Aromaticity of Biochar-Manure: Insights from Elemental, Stable Isotope and Solid-State DPMAS 13C NMR Analyses. *J. Environ. Manage.* **2021**, *280*, 111705. https://doi.org/10.1016/j.jenvman.2020.111705.
111. Deng, W.; Kuang, X.; Xu, Z.; Li, D.; Li, Y.; Zhang, Y. Adsorption of Cadmium and Lead Capacity and Environmental Stability of Magnesium-Modified High-Sulfur Hydrochar: Greenly Utilizing Chicken Feather. *Toxics* **2024**, *12*, 356. https://doi.org/10.3390/toxics12050356.
112. Banik, C.; Bakshi, S.; Andersen, D.S.; Cady, S.D.; Smith, R.G.; Brown, R.C. Does Biochar Stabilize the Bioreactive Carbon Fractions of Swine Manure? *ACS ES&T Eng.* **2023**, *3*, 1212–1226. https://doi.org/10.1021/acsestengg.3c00027.
113. Bin Mobarak, M.; Pinky, N.S.; Mustafi, S.; Chowdhury, F.; Nahar, A.; Akhtar, U.S.; Quddus, M.S.; Yasmin, S.; Alam, M.A. Unveiling the Reactor Effect: A Comprehensive Characterization of Biochar Derived from Rubber Seed Shell via Pyrolysis and in-House Reactor. *RSC Adv.* **2024**, *14*, 29848–29859. https://doi.org/10.1039/d4ra05562d.
114. Zhang, S.; Jia, X.; Wang, X.; Chen, J.; Cheng, C.; Jia, X.; Hu, H. Using the Conditional Process Analysis Model to Characterize the Evolution of Carbon Structure in Taxodium Ascendens Biochar with Varied Pyrolysis Temperature and Holding Time. *Plants* **2024**, *13*, 460. https://doi.org/10.3390/plants13030460.
115. Yang, H.; Yu, Y.; Zhang, H.; Wang, W.; Zhu, J.; Chen, Y.; Zhang, S.; Chen, H. Effect Mechanism of Phosphorous-Containing Additives on Carbon Structure Evolution and Biochar Stability Enhancement. *Biochar* **2024**, *6*, 39. https://doi.org/10.1007/s42773-024-00330-5.
116. Hwang, H.; Sahin, O.; Choi, J.W. Manufacturing a Super-Active Carbon Using Fast Pyrolysis Char from Biomass and Correlation Study on Structural Features and Phenol Adsorption. *RSC Adv.* **2017**, *7*, 42192–42202. https://doi.org/10.1039/c7ra06910c.
117. Wang, S.; Jiang, D.; Cao, B.; Qian, L.; Hu, Y.; Liu, L.; Yuan, C.; Abomohra, A.E.F.; He, Z.; Wang, Q.; et al. Bio-Char and Bio-Oil Characteristics Produced from the Interaction of Enteromorpha Clathrate Volatiles and Rice Husk Bio-Char during Co-Pyrolysis in a Sectional Pyrolysis Furnace: A Complementary Study. *J. Anal. Appl. Pyrolysis* **2018**, *135*, 219–230. https://doi.org/10.1016/j.jaap.2018.08.030.
118. Wang, S.; Wu, L.; Hu, X.; Zhang, L.; O'Donnell, K.M.; Buckley, C.E.; Li, C.Z. An X-Ray Photoelectron Spectroscopic Perspective for the Evolution of O-Containing Structures in Char during Gasification. *Fuel Process. Technol.* **2018**, *172*, 209–215. https://doi.org/10.1016/j.fuproc.2017.12.019.
119. Chen, J.; Zhao, M.; Nawaz Khan, S.; Liu, Y.; Zhao, S.; Dong, W.; Song, Q.; Wang, C. Deeper Insights into the Devolatilization Mechanism of Biomass Fixed-Bed Gasification under Various Atmospheres. *Energy Convers. Manag.* **2024**, *322*, 119113. https://doi.org/10.1016/j.enconman.2024.119113.
120. Chen, T.; Zhang, J.; Wang, Z.; Zhao, R.; He, J.; Wu, J.; Qin, J. Oxygen-Enriched Gasification of Lignocellulosic Biomass: Syngas Analysis, Physicochemical Characteristics of the Carbon-Rich Material and Its Utilization as an Anode in Lithium Ion Battery. *Energy* **2020**, *212*, 118771. https://doi.org/10.1016/j.energy.2020.118771.
121. Del Grosso, M.; Cutz, L.; Tiringer, U.; Tsekos, C.; Taheri, P.; de Jong, W. Influence of Indirectly Heated Steam-Blown Gasification Process Conditions on Biochar Physico-Chemical Properties. *Fuel Process. Technol.* **2022**, *235*, 107347. https://doi.org/10.1016/j.fuproc.2022.107347.
122. Guizani, C.; Jeguirim, M.; Valin, S.; Limousy, L.; Salvador, S. Biomass Chars: The Effects of Pyrolysis Conditions on Their Morphology, Structure, Chemical Properties and Reactivity. *Energies* **2017**, *10*, 796. https://doi.org/10.3390/en10060796.
123. Asadullah, M.; Zhang, S.; Li, C.Z. Evaluation of Structural Features of Chars from Pyrolysis of Biomass of Different Particle Sizes. *Fuel Process. Technol.* **2010**, *91*, 877–881. https://doi.org/10.1016/j.fuproc.2009.08.008.

124. Xu, J.; Liu, J.; Ling, P.; Zhang, X.; Xu, K.; He, L.; Wang, Y.; Su, S.; Hu, S.; Xiang, J. Raman Spectroscopy of Biochar from the Pyrolysis of Three Typical Chinese Biomasses: A Novel Method for Rapidly Evaluating the Biochar Property. *Energy* **2020**, *202*, 117644. https://doi.org/10.1016/j.energy.2020.117644.
125. Azargohar, R.; Nanda, S.; Kozinski, J.A.; Dalai, A.K.; Sutarto, R. Effects of Temperature on the Physicochemical Characteristics of Fast Pyrolysis Bio-Chars Derived from Canadian Waste Biomass. *Fuel* **2014**, *125*, 90–100. https://doi.org/10.1016/j.fuel.2014.01.083.
126. Naim, W.; Treu, P.; Dohrn, M.; Saraçi, E.; Grunwaldt, J.D.; Fendt, S.; Spliethoff, H. Structure-Reactivity- and Modelling-Relationships during Thermal Annealing in Biomass Entrained-Flow Gasification: The Effect of Temperature and Residence Time. *Fuel* **2025**, *383*, 133848. https://doi.org/10.1016/j.fuel.2024.133848.
127. Gao, W.; Liang, S.; Wang, R.; Jiang, Q.; Zhang, Y.; Zheng, Q.; Xie, B.; Toe, C.Y.; Zhu, X.; Wang, J.; et al. Industrial Carbon Dioxide Capture and Utilization: State of the Art and Future Challenges. *Chem. Soc. Rev.* **2020**, *49*, 8584–8686. https://doi.org/10.1039/d0cs00025f.
128. Medina-Martos, E.; Gálvez-Martos, J.L.; Almarza, J.; Lirio, C.; Iribarren, D.; Valente, A.; Dufour, J. Environmental and Economic Performance of Carbon Capture with Sodium Hydroxide. *J. CO_2 Util.* **2022**, *60*, 101991. https://doi.org/10.1016/j.jcou.2022.101991.
129. Rehman, A.; Park, S.J. Tunable Nitrogen-Doped Microporous Carbons: Delineating the Role of Optimum Pore Size for Enhanced CO_2 Adsorption. *Chem. Eng. J.* **2019**, *362*, 731–742. https://doi.org/10.1016/j.cej.2019.01.063.
130. Su, G.; Yang, S.; Jiang, Y.; Li, J.; Li, S.; Ren, J.C.; Liu, W. Modeling Chemical Reactions on Surfaces: The Roles of Chemical Bonding and van Der Waals Interactions. *Prog. Surf. Sci.* **2019**, *94*, 100561. https://doi.org/10.1016/j.progsurf.2019.100561.
131. Yu, S.; Bo, J.; Fengli, L.; Jiegang, L. Structure and Fractal Characteristic of Micro- and Meso-Pores in Low, Middle-Rank Tectonic Deformed Coals by CO_2 and N_2 Adsorption. *Microporous Mesoporous Mater.* **2017**, *253*, 191–202. https://doi.org/10.1016/j.micromeso.2017.07.009.
132. Zhang, Z.; Zhou, J.; Xing, W.; Xue, Q.; Yan, Z.; Zhuo, S.; Qiao, S.Z. Critical Role of Small Micropores in High CO_2 Uptake. *Phys. Chem. Chem. Phys.* **2013**, *15*, 2523–2529. https://doi.org/10.1039/c2cp44436d.
133. Bell, J.G.; Benham, M.J.; Thomas, K.M. Adsorption of Carbon Dioxide, Water Vapor, Nitrogen, and Sulfur Dioxide on Activated Carbon for Capture from Flue Gases: Competitive Adsorption and Selectivity Aspects. *Energy Fuels* **2021**, *35*, 8102–8116. https://doi.org/10.1021/acs.energyfuels.1c00339.
134. Vorokhta, M.; Kusdhany, M.I.M.; Švábová, M.; Nishihara, M.; Sasaki, K.; Lyth, S.M. Hierarchically Porous Carbon Foams Coated with Carbon Nitride: Insights into Adsorbents for Pre-Combustion and Post-Combustion CO_2 Separation. *Sep. Purif. Technol.* **2025**, *354 Pt 5*, 129054. https://doi.org/10.1016/j.seppur.2024.129054.
135. Yu, H.; Xu, H.; Fan, J.; Zhu, Y.B.; Wang, F.; Wu, H. Transport of Shale Gas in Microporous/Nanoporous Media: Molecular to Pore-Scale Simulations. *Energy Fuels* **2021**, *35*, 911–943. https://doi.org/10.1021/acs.energyfuels.0c03276.
136. Li, W.; Liu, J.; Zhao, D. Mesoporous Materials for Energy Conversion and Storage Devices. *Nat. Rev. Mater.* **2016**, *1*, 16023. https://doi.org/10.1038/natrevmats.2016.23.
137. Hijazi, N.; Bavykina, A.; Yarulina, I.; Shoinkhorova, T.; Ramos-Fernandez, E.V.; Gascon, J. Chemical Engineering of Zeolites: Alleviating Transport Limitations through Hierarchical Design and Shaping. *Chem. Soc. Rev.* **2025**, *54*, 6335–6384. https://doi.org/10.1039/d5cs00169b.
138. Sun, M.H.; Huang, S.Z.; Chen, L.H.; Li, Y.; Yang, X.Y.; Yuan, Z.Y.; Su, B.L. Applications of Hierarchically Structured Porous Materials from Energy Storage and Conversion, Catalysis, Photocatalysis, Adsorption, Separation, and Sensing to Biomedicine. *Chem. Soc. Rev.* **2016**, *45*, 3479–3563. https://doi.org/10.1039/c6cs00135a.
139. Petrovic, B.; Gorbounov, M.; Masoudi Soltani, S. Influence of Surface Modification on Selective CO_2 Adsorption: A Technical Review on Mechanisms and Methods. *Microporous Mesoporous Mater.* **2021**, *312*, 110751. https://doi.org/10.1016/j.micromeso.2020.110751.
140. Sun, G.D.; Cao, Y.N.; Hu, M.Z.; Liang, X.H.; Wang, Z.; Cai, Z.J.; Shen, F.Y.; He, H.; Wang, Z.X.; Zhou, K. Bin Pyrrolic N-Doped Carbon Catalysts for Highly Efficient Electrocatalytic Reduction of CO_2 with Superior CO Selectivity over a Wide Potential Window. *Carbon N. Y.* **2023**, *214*, 118320. https://doi.org/10.1016/j.carbon.2023.118320.
141. Guo, J.; Lu, D.; Chen, P.; Zhu, H.; Li, B.; Li, S.; Zhang, C.; Dong, Z.; Cong, Y.; Li, X. Evolution of Sulfur Chemical Morphology of Petroleum Pitches on Their Mesophase Transformation Behaviors and Microcrystalline Structure of the Derived Artificial Graphite. *J. Anal. Appl. Pyrolysis* **2025**, *191*, 107189. https://doi.org/10.1016/j.jaap.2025.107189.
142. Liu, W.J.; Jiang, H.; Yu, H.Q. Development of Biochar-Based Functional Materials: Toward a Sustainable Platform Carbon Material. *Chem. Rev.* **2015**, *115*, 12251–12285. https://doi.org/10.1021/acs.chemrev.5b00195.

143. Collins, J.; Gourdin, G.; Foster, M.; Qu, D. Carbon Surface Functionalities and SEI Formation during Li Intercalation. *Carbon N. Y.* **2015**, *92*, 193–244. https://doi.org/10.1016/j.carbon.2015.04.007.
144. Keiluweit, M.; Kleber, M. Molecular-Level Interactions in Soils and Sediments: The Role of Aromatic π-Systems. *Environ. Sci. Technol.* **2009**, *43*, 3421–3429. https://doi.org/10.1021/es8033044.
145. Kobaisi, M.A.; Bhosale, S.V.S.V.; Latham, K.; Raynor, A.M.; Bhosale, S.V.S. V. Functional Naphthalene Diimides: Synthesis, Properties, and Applications. *Chem. Rev.* **2016**, *116*, 11685–11796. https://doi.org/10.1021/acs.chemrev.6b00160.
146. Adeniyi, A.G.; Iwuozor, K.O.; Emenike, E.C.; Sagboye, P.A.; Micheal, K.T.; Micheal, T.T.; Saliu, O.D.; James, R. Biomass-Derived Activated Carbon Monoliths: A Review of Production Routes, Performance, and Commercialization Potential. *J. Clean. Prod.* **2023**, *423*, 138711. https://doi.org/10.1016/j.jclepro.2023.138711.
147. Kundu, S.; Khandaker, T.; Anik, M.A.A.M.; Hasan, M.K.; Dhar, P.K.; Dutta, S.K.; Latif, M.A.; Hossain, M.S. A Comprehensive Review of Enhanced CO_2 Capture Using Activated Carbon Derived from Biomass Feedstock. *RSC Adv.* **2024**, *14*, 29693–29736. https://doi.org/10.1039/d4ra04537h.
148. Wang, J.; Kaskel, S. KOH Activation of Carbon-Based Materials for Energy Storage. *J. Mater. Chem.* **2012**, *22*, 23710–23725. https://doi.org/10.1039/c2jm34066f.
149. Abdel-Shafy, H.I.; Ibrahim, A.M.; Al-Sulaiman, A.M.; Okasha, R.A. Landfill Leachate: Sources, Nature, Organic Composition, and Treatment: An Environmental Overview. *Ain Shams Eng. J.* **2024**, *15*, 102293. https://doi.org/10.1016/j.asej.2023.102293.
150. Caliman, F.A.; Robu, B.M.; Smaranda, C.; Pavel, V.L.; Gavrilescu, M. Soil and Groundwater Cleanup: Benefits and Limits of Emerging Technologies. *Clean Technol. Environ. Policy* **2011**, *13*, 241–268. https://doi.org/10.1007/s10098-010-0319-z.
151. Alammar, A.Y.; Choi, S.H.; Buonomenna, M.G. Hollow Fiber Membrane Modification by Interfacial Polymerization for Organic Solvent Nanofiltration. *Processes* **2024**, *12*, 563. https://doi.org/10.3390/pr12030563.
152. Mahbub, P.; Duke, M. Scalability of Advanced Oxidation Processes (AOPs) in Industrial Applications: A Review. *J. Environ. Manage.* **2023**, *345*, 118861. https://doi.org/10.1016/j.jenvman.2023.118861.
153. Pet, I.; Sanad, M.N.; Farouz, M.; ElFaham, M.M.; El-Hussein, A.; El-sadek, M.S.A.; Althobiti, R.A.; Ioanid, A. Review: Recent Developments in the Implementation of Activated Carbon as Heavy Metal Removal Management. *Water Conserv. Sci. Eng.* **2024**, *9*, 62. https://doi.org/10.1007/s41101-024-00287-3.
154. Leng, L.; Yang, L.; Lei, X.; Zhang, W.; Ai, Z.; Yang, Z.; Zhan, H.; Yang, J.; Yuan, X.; Peng, H.; et al. Machine Learning Predicting and Engineering the Yield, N Content, and Specific Surface Area of Biochar Derived from Pyrolysis of Biomass. *Biochar* **2022**, *4*, 63. https://doi.org/10.1007/s42773-022-00183-w.
155. Li, X.; Huang, Z.; Shao, S.; Cai, Y. Machine Learning Prediction of Physical Properties and Nitrogen Content of Porous Carbon from Agricultural Wastes: Effects of Activation and Doping Process. *Fuel* **2024**, *356*, 129623. https://doi.org/10.1016/j.fuel.2023.129623.
156. Liu, D.J.; Garcia, A.; Wang, J.; Ackerman, D.M.; Wang, C.J.; Evans, J.W. Kinetic Monte Carlo Simulation of Statistical Mechanical Models and Coarse-Grained Mesoscale Descriptions of Catalytic Reaction-Diffusion Processes: 1D Nanoporous and 2D Surface Systems. *Chem. Rev.* **2015**, *115*, 5979–6050. https://doi.org/10.1021/cr500453t.
157. Torrisi, A.; Bell, R.G.; Mellot-Draznieks, C. Predicting the Impact of Functionalized Ligands on CO_2 Adsorption in MOFs: A Combined DFT and Grand Canonical Monte Carlo Study. *Microporous Mesoporous Mater.* **2013**, *168*, 225–238. https://doi.org/10.1016/j.micromeso.2012.10.002.
158. Habibur Rahman Sobuz, M.; Khan, M.H.; Kawsarul Islam Kabbo, M.; Alhamami, A.H.; Aditto, F.S.; Saziduzzaman Sajib, M.; Johnson Alengaram, U.; Mansour, W.; Hasan, N.M.S.; Datta, S.D.; et al. Assessment of Mechanical Properties with Machine Learning Modeling and Durability, and Microstructural Characteristics of a Biochar-Cement Mortar Composite. *Constr. Build. Mater.* **2024**, *411*, 134281. https://doi.org/10.1016/j.conbuildmat.2023.134281.
159. Li, J.; Pan, L.; Suvarna, M.; Tong, Y.W.; Wang, X. Fuel Properties of Hydrochar and Pyrochar: Prediction and Exploration with Machine Learning. *Appl. Energy* **2020**, *269*, 115166. https://doi.org/10.1016/j.apenergy.2020.115166.
160. Duan, L.; Wang, C.; Zhang, W.; Ma, B.; Deng, Y.; Li, W.; Zhao, D. Interfacial Assembly and Applications of Functional Mesoporous Materials. *Chem. Rev.* **2021**, *121*, 14349–14429. https://doi.org/10.1021/acs.chemrev.1c00236.
161. Ghosh, S.; Zaid, M.; Dutta, J.; Parvin, M.; Martha, S.K. Soft Carbon in Non-Aqueous Rechargeable Batteries: A Review of Its Synthesis, Carbonization Mechanism, Characterization, and Multifarious Applications. *Energy Adv.* **2024**, *3*, 1167–1195. https://doi.org/10.1039/d4ya00174e.
162. Mochida, I.; Fujimoto, K.; Oyama, T. Chemistry in the Production and Utilization of Needle Coke. In *Chemistry & Physics of Carbon*; CRC Press: Boca Raton, FL, USA, 1993; pp. 111–212, ISBN 9781003418184.

163. Cho, D.W.; Kwon, E.E.; Song, H. Use of Carbon Dioxide as a Reaction Medium in the Thermo-Chemical Process for the Enhanced Generation of Syngas and Tuning Adsorption Ability of Biochar. *Energy Convers. Manag.* **2016**, *117*, 106–114. https://doi.org/10.1016/j.enconman.2016.03.027.
164. Dai, H.; Zhao, H.; Chen, S.; Jiang, B. A Microwave-Assisted Boudouard Reaction: A Highly Effective Reduction of the Greenhouse Gas CO_2 to Useful Co Feedstock with Semi-Coke. *Molecules* **2021**, *26*, 1507. https://doi.org/10.3390/molecules26061507.
165. Hunt, J.; Ferrari, A.; Lita, A.; Crosswhite, M.; Ashley, B.; Stiegman, A.E. Microwave-Specific Enhancement of the Carbon−Carbon Dioxide (Boudouard) Reaction. *J. Phys. Chem. C* **2013**, *117*, 26871–26880. https://doi.org/10.1021/jp4076965.
166. Singh, R.; Wang, L.; Ostrikov, K.; Huang, J. Designing Carbon-Based Porous Materials for Carbon Dioxide Capture. *Adv. Mater. Interfaces* **2024**, *11*, 2202290. https://doi.org/10.1002/admi.202202290.
167. Vidal-Vidal, Á.; Faza, O.N.; Silva López, C. CO_2 Complexes with Five-Membered Heterocycles: Structure, Topology, and Spectroscopic Characterization. *J. Phys. Chem. A* **2017**, *121*, 9118–9130. https://doi.org/10.1021/acs.jpca.7b09394.
168. Alshareef, R.; Nahil, M.A.; Williams, P.T. Hydrogen Production by Three-Stage (i) Pyrolysis, (ii) Catalytic Steam Reforming, and (iii) Water Gas Shift Processing of Waste Plastic. *Energy Fuels* **2023**, *37*, 3894–3907. https://doi.org/10.1021/acs.energyfuels.2c02934.
169. Meshkani, F.; Rezaei, M. High Temperature Water Gas Shift Reaction over Promoted Iron Based Catalysts Prepared by Pyrolysis Method. *Int. J. Hydrog. Energy* **2014**, *39*, 16318–16328. https://doi.org/10.1016/j.ijhydene.2014.07.176.
170. Bordes, A.; Marlair, G.; Zantman, A.; Herreyre, S.; Papin, A.; Desprez, P.; Lecocq, A. New Insight on the Risk Profile Pertaining to Lithium-Ion Batteries under Thermal Runaway as Affected by System Modularity and Subsequent Oxidation Regime. *J. Energy Storage* **2022**, *52 Pt B*, 104790. https://doi.org/10.1016/j.est.2022.104790.
171. Jagtap, S.; Handore, K.; Adhav, P.; Deshpande, P.; Bhopale, A.; Khaladkar, M.; Khandagale, P.; Chabukswar, V.V. Room Temperature Operating, Fast and Reusable Polyaniline Sensor Synthesized Ultrasonically Using Organic and Inorganic Acid Dopants. *J. Macromol. Sci. Part B Phys.* **2022**, *61*, 942–957. https://doi.org/10.1080/00222348.2022.2122236.
172. Lakhal, R.; Almatar, M.; Alkalaf, T.; Albarri, O. Transcriptome-Based Analysis of the Oxidative Response of Thermotoga Maritima to the O_2 Stress. *Comb. Chem. High Throughput Screen.* **2025**, *in press*. https://doi.org/10.2174/0113862073339580241128075031.
173. Samanta, S.; Srivastava, R. Catalytic Conversion of CO_2 to Chemicals and Fuels: The Collective Thermocatalytic/Photocatalytic/Electrocatalytic Approach with Graphitic Carbon Nitride. *Mater. Adv.* **2020**, *1*, 1506–1545. https://doi.org/10.1039/d0ma00293c.
174. Kuang, H.Y.; Lin, Y.X.; Li, X.H.; Chen, J.S. Chemical Fixation of CO_2 on Nanocarbons and Hybrids. *J. Mater. Chem. A* **2021**, *9*, 20857–20873. https://doi.org/10.1039/d1ta05080j.
175. Lin, F.; Xu, M.; Ramasamy, K.K.; Li, Z.; Klinger, J.L.; Schaidle, J.A.; Wang, H. Catalyst Deactivation and Its Mitigation during Catalytic Conversions of Biomass. *ACS Catal.* **2022**, *12*, 13555–13599. https://doi.org/10.1021/acscatal.2c02074.
176. Pota, F.; Costa de Oliveira, M.; Schröder, C.; Brunet Cabré, M.; Nolan, H.; Rafferty, A.; Jeannin, O.; Camerel, F.; Behan, J.; Barrière, F.; et al. Porous N-doped Carbon-encapsulated Iron as a Novel Catalyst Architecture for the Electrocatalytic Hydrogenation of Benzaldehyde. *ChemSusChem* **2024**, *18*, e202400546. https://doi.org/10.1002/cssc.202400546.
177. Raza, A.; Altaf, S.; Ali, S.; Ikram, M.; Li, G. Recent Advances in Carbonaceous Sustainable Nanomaterials for Wastewater Treatments. *Sustain. Mater. Technol.* **2022**, *32*, e00406. https://doi.org/10.1016/j.susmat.2022.e00406.
178. Joseph, S.; Saianand, G.; Benzigar, M.R.; Ramadass, K.; Singh, G.; Anantha-Iyengar Gopalan Jae Hun, Y.; Mori, T.; Al-Muhtaseb, A.H.; Jiabao Yi, A.V. Recent Advances in Functionalized Nanoporous Carbons Derived from Waste Resources and Their Applications in Energy and Environment. *Adv. Sustain. Syst.* **2021**, *5*, 2000169. https://doi.org/10.1002/adsu.202000169.
179. Libra, J.A.; Ro, K.S.; Kammann, C.; Funke, A.; Berge, N.D.; Neubauer, Y.; Titirici, M.M.; Fühner, C.; Bens, O.; Kern, J.; et al. Hydrothermal Carbonization of Biomass Residuals: A Comparative Review of the Chemistry, Processes and Applications of Wet and Dry Pyrolysis. *Biofuels* **2011**, *2*, 71–106. https://doi.org/10.4155/bfs.10.81.
180. Molina, A.; Mondragón, F. Reactivity of Coal Gasification with Steam and CO_2. *Fuel* **1998**, *77*, 1831–1839. https://doi.org/10.1016/S0016-2361(98)00123-9.
181. Lakzian, E.; Yazdani, S.; Salmani, F.; Mahian, O.; Kim, H.D.; Ghalambaz, M.; Ding, H.; Yang, Y.; Li, B.; Wen, C. Supersonic Separation towards Sustainable Gas Removal and Carbon Capture. *Prog. Energy Combust. Sci.* **2024**, *103*, 101158. https://doi.org/10.1016/j.pecs.2024.101158.
182. Risoluti, R.; Gullifa, G.; Barone, L.; Papa, E.; Materazzi, S. On-Line Thermally Induced Evolved Gas Analysis: An Update—Part 1: EGA-MS. *Molecules* **2022**, *27*, 3518. https://doi.org/10.3390/molecules27248926.

183. Mohamed, R.Y.A.; Kumarachari, R.K.; Bukke, S.P.N.; Neerugatti, D.; Mekasha, Y.T.; Bandarapalle, K. Plasma Catalysis for Sustainable Industry: Lab-Scale Studies and Pathways to Upscaling. *Discov. Appl. Sci.* **2025**, *7*, 271. https://doi.org/10.1007/s42452-025-06718-7.
184. Mondal, S.; Ruidas, S.; Chongdar, S.; Saha, B.; Bhaumik, A. Sustainable Porous Heterogeneous Catalysts for the Conversion of Biomass into Renewable Energy Products. *ACS Sustain. Resour. Manag.* **2024**, *1*, 1672–1704. https://doi.org/10.1021/acssusresmgt.4c00190.
185. Xiao, N.; Kong, L.; Wei, M.; Hu, X.; Li, O. Innovations in Food Waste Management: From Resource Recovery to Sustainable Solutions. *Waste Dispos. Sustain. Energy* **2024**, *6*, 401–417. https://doi.org/10.1007/s42768-024-00201-6.
186. Zhang, K.; Guo, D.; Wang, X.; Qin, Y.; Hu, L.; Zhang, Y. Sustainable CO_2 Management through Integrated CO_2 Capture and Conversion. *J. CO_2 Util.* **2023**, *72*, 102493. https://doi.org/10.1016/j.jcou.2023.102493.
187. Razzak, S.A. Municipal Solid and Plastic Waste Co-Pyrolysis Towards Sustainable Renewable Fuel and Carbon Materials: A Comprehensive Review. *Chem. Asian J.* **2024**, *19*, e202400307. https://doi.org/10.1002/asia.202400307.
188. Yuan, X.; Cao, Y.; Li, J.; Patel, A.K.; Dong, C.D.; Jin, X.; Gu, C.; Yip, A.C.K.; Tsang, D.C.W.; Ok, Y.S. Recent Advancements and Challenges in Emerging Applications of Biochar-Based Catalysts. *Biotechnol. Adv.* **2023**, *67*, 108181. https://doi.org/10.1016/j.biotechadv.2023.108181.
189. Chidhambaram, N.; Kay, S.J.J.; Priyadharshini, S.; Meenakshi, R.; Sakthivel, P.; Dhanbalan, S.; Shanavas, S.; Kamaraj, S.K.; Thirumurugan, A. Magnetic Nanomaterials as Catalysts for Syngas Production and Conversion. *Catalysts* **2023**, *13*, 440. https://doi.org/10.3390/catal13020440.
190. Ansari, M.N.M.; Sayem, M.A. Microwave-Assisted Activated Carbon: A Promising Class of Materials for a Wide Range of Applications. In *Radiation Technologies and Applications in Materials Science*; Chowdhury, S.R., Ed.; CRC Press: Boca Raton, FL, USA, 2022; pp. 1–38, ISBN 9788490225370.
191. Zhang, J.; Sewell, C.D.; Huang, H.; Lin, Z. Closing the Anthropogenic Chemical Carbon Cycle toward a Sustainable Future via CO_2 Valorization. *Adv. Energy Mater.* **2021**, *11*, 2102767. https://doi.org/10.1002/aenm.202102767.
192. Mahmoudi Kouhi, R.; Jebrailvand Moghaddam, M.M.; Doulati Ardejani, F.; Mirheydari, A.; Maghsoudy, S.; Gholizadeh, F.; Ghobadipour, B. Carbon Utilization Technologies & Methods. In *Carbon Capture, Utilization, and Storage Technologies Towards More Sustainable Cities*; Ahmadian, A., Elkamel, A., Almansoori, A., Eds.; Springer: Berlin/Heidelberg, Germany, 2024; pp. 1–50, ISBN 978-3-031-46590-1.
193. Chinenye Divine, D.; Hubert, S.; Epelle, E.I.; Ojo, A.U.; Adeleke, A.A.; Ogbaga, C.C.; Akande, O.; Okoye, P.U.; Giwa, A.; Okolie, J.A. Enhancing Biomass Pyrolysis: Predictive Insights from Process Simulation Integrated with Interpretable Machine Learning Models. *Fuel* **2024**, *366*, 131346. https://doi.org/10.1016/j.fuel.2024.131346.
194. Sirohi, R.; Kumar, M.; Vivekanand, V.; Shakya, A.; Tarafdar, A.; Singh, R.; Sawarkar, A.D.; Hoang, A.T.; Pandey, A. Integrating Biochar in Anaerobic Digestion: Insights into Diverse Feedstocks and Algal Biochar. *Environ. Technol. Innov.* **2024**, *36*, 103814. https://doi.org/10.1016/j.eti.2024.103814.
195. Olivier, A.; Desgagnés, A.; Mercier, E.; Iliuta, M.C. New Insights on Catalytic Valorization of Carbon Dioxide by Conventional and Intensified Processes. *Ind. Eng. Chem. Res.* **2023**, *62*, 5714–5749. https://doi.org/10.1021/acs.iecr.3c00064.
196. Wang, Q.; Han, L. Hydrogen Production. In *Handbook of Climate Change Mitigation and Adaptation*; Chen, W.-Y., Suzuki, T., Lackner, M., Eds.; Springer: Cham, Switzerland, 2022; pp. 1855–1900, ISBN 9783319144092.
197. Goel, A.; Moghaddam, E.M.; Liu, W.; He, C.; Konttinen, J. Biomass Chemical Looping Gasification for High-Quality Syngas: A Critical Review and Technological Outlooks. *Energy Convers. Manag.* **2022**, *268*, 116020. https://doi.org/10.1016/j.enconman.2022.116020.
198. Lott, P.; Deutschmann, O. Heterogeneous Chemical Reactions—A Cornerstone in Emission Reduction of Local Pollutants and Greenhouse Gases. *Proc. Combust. Inst.* **2023**, *39*, 3183–3215. https://doi.org/10.1016/j.proci.2022.06.001.
199. Shadle, L.J.; Indrawan, N.; Breault, R.W.; Bennett, J. Gasification Technology. In *Handbook of Climate Change Mitigation and Adaptation*; Lackner, M., Baharak, S., Wei-Yin, C., Eds.; Springer: Berlin/Heidelberg, Germany, 2022; pp. 653–741, ISBN 978-3-030-72578-5.
200. El-Fawal, E.M.; El Naggar, A.M.A.; El-Zahhar, A.A.; Alghandi, M.M.; Morshedy, A.S.; El Sayed, H.A.; Mohammed, A. elshifa M.E. Biofuel Production from Waste Residuals: Comprehensive Insights into Biomass Conversion Technologies and Engineered Biochar Applications. *RSC Adv.* **2025**, *15*, 11942–11974. https://doi.org/10.1039/d5ra00857c.
201. Kasipandi, S.; Bae, J.W. Recent Advances in Direct Synthesis of Value-Added Aromatic Chemicals from Syngas by Cascade Reactions over Bifunctional Catalysts. *Adv. Mater.* **2019**, *31*, 1803390. https://doi.org/10.1002/adma.201803390.

202. Santos, R.G.d.; Alencar, A.C. Biomass-Derived Syngas Production via Gasification Process and Its Catalytic Conversion into Fuels by Fischer Tropsch Synthesis: A Review. *Int. J. Hydrog. Energy* **2020**, *45*, 18114–18132. https://doi.org/10.1016/j.ijhydene.2019.07.133.
203. Gao, S.; Song, Z.; Sun, H.; Zhang, Y.Y.; Ma, J.; Zhang, Y.Y. Progress of Oxygen Generation Technologies in High-Altitude and Emergency Rescue Conditions. *Asia-Pac. J. Chem. Eng.* **2025**, e70040. https://doi.org/10.1002/APJ.70040.
204. Ghasemi, A.; Nikafshan Rad, H.; Izadyar, N.; Marefati, M. Optimizing Industrial Energy: An Eco-Efficient System for Integrated Power, Oxygen, and Methanol Production Using Coke Plant Waste Heat and Electrolysis. *Energy Convers. Manag. X* **2024**, *22*, 100571. https://doi.org/10.1016/j.ecmx.2024.100571.
205. Bhatia, M.; Gugnani, R.; Yaqub, M.Z.; Agarwal, V. Drivers and Challenges in Achieving Corporate Carbon Neutrality—Qualitative Investigation of Carbon Capture, Utilization, and Storage Technologies. *Bus. Strateg. Environ.* **2024**, *34*, 1771–1791. https://doi.org/10.1002/bse.4068.
206. Liu, Y.; Paskevicius, M.; Sofianos, M.V.; Parkinson, G.; Wang, S.; Li, C.Z. A SAXS Study of the Pore Structure Evolution in Biochar during Gasification in H_2O, CO_2 and H_2O/CO_2. *Fuel* **2021**, *292*, 120384. https://doi.org/10.1016/j.fuel.2021.120384.
207. Ravenni, G.; Elhami, O.H.; Ahrenfeldt, J.; Henriksen, U.B.; Neubauer, Y. Adsorption and Decomposition of Tar Model Compounds over the Surface of Gasification Char and Active Carbon within the Temperature Range 250–800 °C. *Appl. Energy* **2019**, *241*, 139–151. https://doi.org/10.1016/j.apenergy.2019.03.032.
208. Sneddon, G.; Greenaway, A.; Yiu, H.H.P. The Potential Applications of Nanoporous Materials for the Adsorption, Separation, and Catalytic Conversion of Carbon Dioxide. *Adv. Energy Mater.* **2014**, *4*, 1301873. https://doi.org/10.1002/aenm.201301873.
209. Ciccone, B.; Murena, F.; Ruoppolo, G.; Urciuolo, M.; Brachi, P. Methanation of Syngas from Biomass Gasification: Small-Scale Plant Design in Aspen Plus. *Appl. Therm. Eng.* **2024**, *246*, 122901. https://doi.org/10.1016/j.applthermaleng.2024.122901.
210. Gao, K.; Chen, G.; Yan, B.; Ti, S.; Wang, H.; Si, G.; Qi, T. Modeling of Biomass Thermal Decomposition/Gasification in a Downdraft Gasifier under Low Pressure by Aspen Plus. *Therm. Sci. Eng. Prog.* **2025**, *59*, 103229. https://doi.org/10.1016/j.tsep.2025.103229.
211. Materazzi, M.; Lettieri, P.; Mazzei, L.; Taylor, R.; Chapman, C. Tar Evolution in a Two Stage Fluid Bed-Plasma Gasification Process for Waste Valorization. *Fuel Process. Technol.* **2014**, *128*, 146–157. https://doi.org/10.1016/j.fuproc.2014.06.028.
212. Cinti, G.; Baldinelli, A.; Di Michele, A.; Desideri, U. Integration of Solid Oxide Electrolyzer and Fischer-Tropsch: A Sustainable Pathway for Synthetic Fuel. *Appl. Energy* **2016**, *162*, 308–320. https://doi.org/10.1016/j.apenergy.2015.10.053.
213. Alsunousi, M.; Kayabasi, E. The Role of Hydrogen in Synthetic Fuel Production Strategies. *Int. J. Hydrog. Energy* **2024**, *54*, 1169–1178. https://doi.org/10.1016/j.ijhydene.2023.11.359.
214. Galán-Martín, Á.; Tulus, V.; Díaz, I.; Pozo, C.; Pérez-Ramírez, J.; Guillén-Gosálbez, G. Sustainability Footprints of a Renewable Carbon Transition for the Petrochemical Sector within Planetary Boundaries. *One Earth* **2021**, *4*, 565–583. https://doi.org/10.1016/j.oneear.2021.04.001.
215. Prifti, K.; Lechtenberg, F.; Manenti, F.; Espuña, A.; Graells, M. Comparing the Climate Impact of Methanol Production in Europe: Steam Methane Reforming vs. Plastic Waste Gasification Processes. *Resour. Conserv. Recycl.* **2024**, *208*, 107653. https://doi.org/10.1016/j.resconrec.2024.107653.
216. Faheem, M.; Azher Hassan, M.; Du, J.; Wang, B. Harnessing Potential of Smart and Conventional Spent Adsorbents: Global Practices and Sustainable Approaches through Regeneration and Tailored Recycling. *Sep. Purif. Technol.* **2025**, *354 Pt 3*, 128907. https://doi.org/10.1016/j.seppur.2024.128907.
217. Patra, N.; Ramesh, P.; Țălu, S. Advancements in Cellulose-Based Materials for CO_2 Capture and Conversion. *Polymers* **2025**, *17*, 848. https://doi.org/10.3390/polym17070848.
218. Sultana, S.; Rahaman, M.; Hassan, A.; Parvez, M.A.; Chandan, M.R. Biomass-Based Sustainable Graphene for Advanced Electronic Technology: A Review. *Chem. Asian J.* **2025**, *20*, e202500128. https://doi.org/10.1002/asia.202500128.
219. Wang, L.; Wang, T.; Hao, R.; Wang, Y. Synthesis and Applications of Biomass-Derived Porous Carbon Materials in Energy Utilization and Environmental Remediation. *Chemosphere* **2023**, *339*, 139635. https://doi.org/10.1016/j.chemosphere.2023.139635.
220. Beak, S.; Kim, S.; Oh, S.; Bae, J. Lignin-Based Porous Carbon for Efficient Hydrogen Storage. *J. Environ. Chem. Eng.* **2025**, *13*, 116086. https://doi.org/10.1016/j.jece.2025.116086.
221. Wang, Q.; Luo, B.; Wang, Z.; Hu, Y.; Du, M. Pore Engineering in Biomass-Derived Carbon Materials for Enhanced Energy, Catalysis, and Environmental Applications. *Molecules* **2024**, *29*, 5172. https://doi.org/10.3390/molecules29215172.
222. Ghosh, S.K.; Ghosh, M. Post-Combustion Capture of Carbon Dioxide by Natural and Synthetic Organic Polymers. *Polysaccharides* **2023**, *4*, 156–175. https://doi.org/10.3390/polysaccharides4020012.

223. Liu, Y.; Wilcox, J. Molecular Simulation Studies of CO_2 Adsorption by Carbon Model Compounds for Carbon Capture and Sequestration Applications. *Environ. Sci. Technol.* **2013**, *47*, 95–101. https://doi.org/10.1021/es3012029.
224. Tiwari, I.; Sharma, P.; Nebhani, L. Polybenzoxazine—An Enticing Precursor for Engineering Heteroatom-Doped Porous Carbon Materials with Applications beyond Energy, Environment and Catalysis. *Mater. Today Chem.* **2022**, *23*, 100734. https://doi.org/10.1016/j.mtchem.2021.100734.
225. Etim, U.J.; Zhang, C.; Zhong, Z. Impacts of the Catalyst Structures on CO_2 Activation on Catalyst Surfaces. *Nanomaterials* **2021**, *11*, 3265. https://doi.org/10.3390/nano11123265.
226. López-Periago, A.M.; Domingo, C. Features of Supercritical CO_2 in the Delicate World of the Nanopores. *J. Supercrit. Fluids* **2018**, *134*, 204–213. https://doi.org/10.1016/j.supflu.2017.11.011.
227. Yin, H.; Zhou, J.; Jiang, Y.; Xian, X.; Liu, Q. Physical and Structural Changes in Shale Associated with Supercritical CO_2 Exposure. *Fuel* **2016**, *184*, 289–303. https://doi.org/10.1016/j.fuel.2016.07.028.
228. Ren, X.; Shanb Ghazani, M.; Zhu, H.; Ao, W.; Zhang, H.; Moreside, E.; Zhu, J.; Yang, P.; Zhong, N.; Bi, X. Challenges and Opportunities in Microwave-Assisted Catalytic Pyrolysis of Biomass: A Review. *Appl. Energy* **2022**, *315*, 118970. https://doi.org/10.1016/j.apenergy.2022.118970.
229. Zhang, Z.; Cano, Z.P.; Luo, D.; Dou, H.; Yu, A.; Chen, Z. Rational Design of Tailored Porous Carbon-Based Materials for CO_2 Capture. *J. Mater. Chem. A* **2019**, *7*, 20985–21003. https://doi.org/10.1039/c9ta07297g.
230. Roy, S.; Das, T.; Dasgupta Ghosh, B.; Goh, K.L.; Sharma, K.; Chang, Y.W. From Hazardous Waste to Green Applications: Selective Surface Functionalization of Waste Cigarette Filters for High-Performance Robust Triboelectric Nanogenerators and CO_2 Adsorbents. *ACS Appl. Mater. Interfaces* **2022**, *14*, 31973–31985. https://doi.org/10.1021/acsami.2c06463.
231. Wang, X.; Chen, Y.; Lindbråthen, A.; Waris, Z.; Deng, L. High Capacity and Robust Moisture-Swing CO_2 Adsorption for Direct Air Capture by Functionalized Cellulose Aerogels. *Chem. Eng. J.* **2025**, *512*, 162377. https://doi.org/10.1016/j.cej.2025.162377.
232. Hardiagon, A.; Coudert, F.X. Multiscale Modeling of Physical Properties of Nanoporous Frameworks: Predicting Mechanical, Thermal, and Adsorption Behavior. *Acc. Chem. Res.* **2024**, *57*, 1620–1632. https://doi.org/10.1021/acs.accounts.4c00161.
233. Sabatino, F.; Grimm, A.; Gallucci, F.; van Sint Annaland, M.; Kramer, G.J.; Gazzani, M. A Comparative Energy and Costs Assessment and Optimization for Direct Air Capture Technologies. *Joule* **2021**, *5*, 2047–2076. https://doi.org/10.1016/j.joule.2021.05.023.
234. Realmonte, G.; Drouet, L.; Gambhir, A.; Glynn, J.; Hawkes, A.; Köberle, A.C.; Tavoni, M. An Inter-Model Assessment of the Role of Direct Air Capture in Deep Mitigation Pathways. *Nat. Commun.* **2019**, *10*, 3277. https://doi.org/10.1038/s41467-019-10842-5.
235. Zolfaghari, Z.; Aslani, A.; Moshari, A.; Malekli, M. Direct Air Capture from Demonstration to Commercialization Stage: A Bibliometric Analysis. *Int. J. Energy Res.* **2022**, *46*, 383–396. https://doi.org/10.1002/er.7203.
236. Fasihi, M.; Efimova, O.; Breyer, C. Techno-Economic Assessment of CO_2 Direct Air Capture Plants. *J. Clean. Prod.* **2019**, *224*, 957–980. https://doi.org/10.1016/j.jclepro.2019.03.086.
237. Wang, X.; Chen, Y.; Xu, W.; Lindbråthen, A.; Cheng, X.; Chen, X.; Zhu, L.; Deng, L. Development of High Capacity Moisture-Swing DAC Sorbent for Direct Air Capture of CO_2. *Sep. Purif. Technol.* **2023**, *324*, 124489. https://doi.org/10.1016/j.seppur.2023.124489.
238. Bouter, A.; Hurtig, O.; Besseau, R.; Buffi, M.; Kulisic, B.; Scarlat, N. Updating the Greenhouse Gas Emissions of Liquid Biofuels from Annex V of the Renewable Energy Directive II (RED II): An Overview. *Biomass Bioenergy* **2025**, *199*, 107886. https://doi.org/10.1016/j.biombioe.2025.107886.
239. Zaker, A.; ben Hammouda, S.; Sun, J.; Wang, X.; Li, X.; Chen, Z. Carbon-Based Materials for CO_2 Capture: Their Production, Modification and Performance. *J. Environ. Chem. Eng.* **2023**, *11*, 109741. https://doi.org/10.1016/j.jece.2023.109741.
240. Zhang, C.; Sun, S.; He, S.; Wu, C. Direct Air Capture of CO_2 by KOH-Activated Bamboo Biochar. *J. Energy Inst.* **2022**, *105*, 399–405. https://doi.org/10.1016/j.joei.2022.10.017.
241. Quan, C.; Zhou, Y.; Gao, N.; Yang, T.; Wang, J.; Wu, C. Direct CO_2 Capture from Air Using Char from Pyrolysis of Digestate Solid. *Biomass Bioenergy* **2023**, *175*, 106891. https://doi.org/10.1016/j.biombioe.2023.106891.
242. Monteagudo, J.M.; Durán, A.; Alonso, M.; Stoica, A.I. Investigation of Effectiveness of KOH-Activated Olive Pomace Biochar for Efficient Direct Air Capture of CO_2. *Sep. Purif. Technol.* **2025**, *352*, 127997. https://doi.org/10.1016/j.seppur.2024.127997.
243. Podder, S.; Jungi, H.; Mitra, J. In Pursuit of Carbon Neutrality: Progresses and Innovations in Sorbents for Direct Air Capture of CO_2. *Chem. A Eur. J.* **2025**, *31*, e202500865. https://doi.org/10.1002/chem.202500865.
244. Zhang, Y.; Ding, L.; Xie, Z.; Zhang, X.; Sui, X.; Li, J.-R. Porous Sorbents for Direct Capture of Carbon Dioxide from Ambient Air. *Chin. Chem. Lett.* **2024**, *36*, 109676. https://doi.org/10.1016/j.cclet.2024.109676.

245. Okonkwo, E.C.; AlNouss, A.; Shahbaz, M.; Al-Ansari, T. Developing Integrated Direct Air Capture and Bioenergy with Carbon Capture and Storage Systems: Progress towards 2 °C and 1.5 °C Climate Goals. *Energy Convers. Manag.* **2023**, *296*, 117687. https://doi.org/10.1016/j.enconman.2023.117687.
246. Küng, L.; Aeschlimann, S.; Charalambous, C.; McIlwaine, F.; Young, J.; Shannon, N.; Strassel, K.; Maesano, C.N.; Kahsar, R.; Pike, D.; et al. A Roadmap for Achieving Scalable, Safe, and Low-Cost Direct Air Carbon Capture and Storage. *Energy Environ. Sci.* **2023**, *16*, 4280–4304. https://doi.org/10.1039/d3ee01008b.
247. Izikowitz, D. Carbon Purchase Agreements, Dactories, and Supply-Chain Innovation: What Will It Take to Scale-Up Modular Direct Air Capture Technology to a Gigatonne Scale. *Front. Clim.* **2021**, *3*, 636657. https://doi.org/10.3389/fclim.2021.636657.